LASERY

HeNe Laser

Výhody He-Ne laseru

Long laser lifetime

unbeatable price–performance ratio

excellent beam quality,,

Excellent mode purity, typical > 95% Gaussian TEM_{00}

A favorable relation between resonator length and resonator width (diameter)

A nearly diffraction-limited beam

High beam-pointing stability

High reproducibility in manufacturing

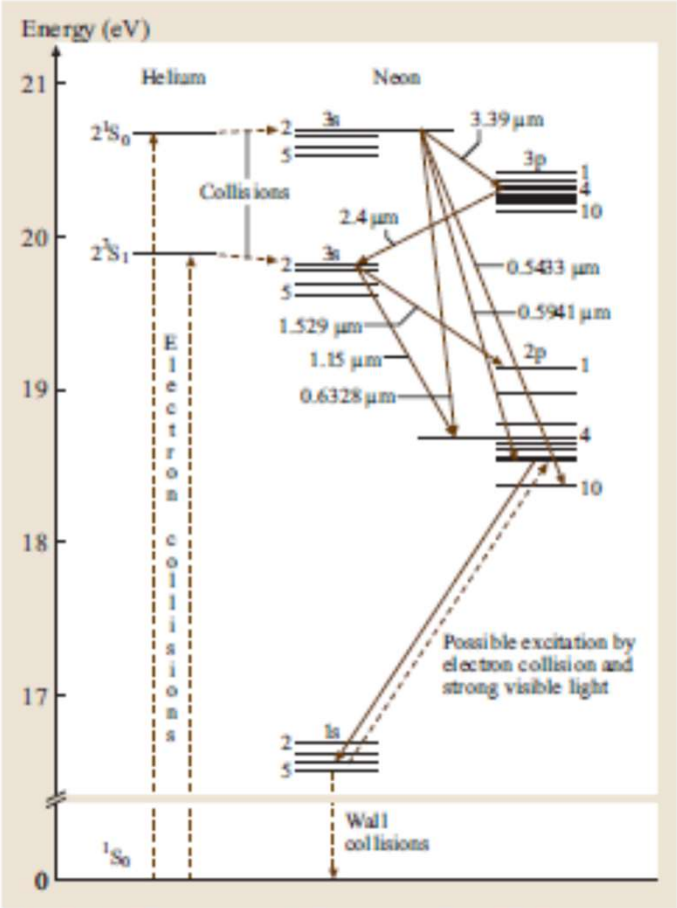

Fig. 11.149 Energy-level diagram of the HeNe laser

Wavelength (in air) (nm)	Transition	Gain (m^{-1})	Typical power (mW)
543.3	$3s_2$–$2p_{10}$	0.03	0.5–3.0
594.1	$3s_2$–$2p_8$		2.0
611.8	$3s_2$–$2p_6$	0.1	2.0
632.8	$3s_2$–$2p_4$	0.5	0.5–50
640.2	$3s_2$–$2p_2$		
1152.3	$2s_2$–$2p_4$		2.0
1523.1	$2s_2$–$2p_1$	4	1
3391.3	$3s_2$–$3p_4$	100	10

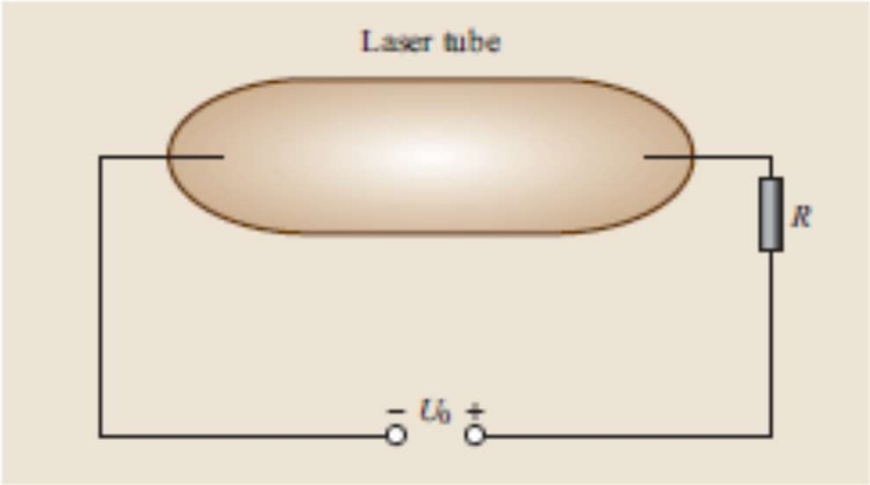

Směs He-Ne, tlak 4-7 mbar, He:Ne…. 5:1 – 10:1

Proud DC, 3 – 11 mA, U = 1 - 5 kV (studený výboj, v kapiláře 0.5 – 2 mm)

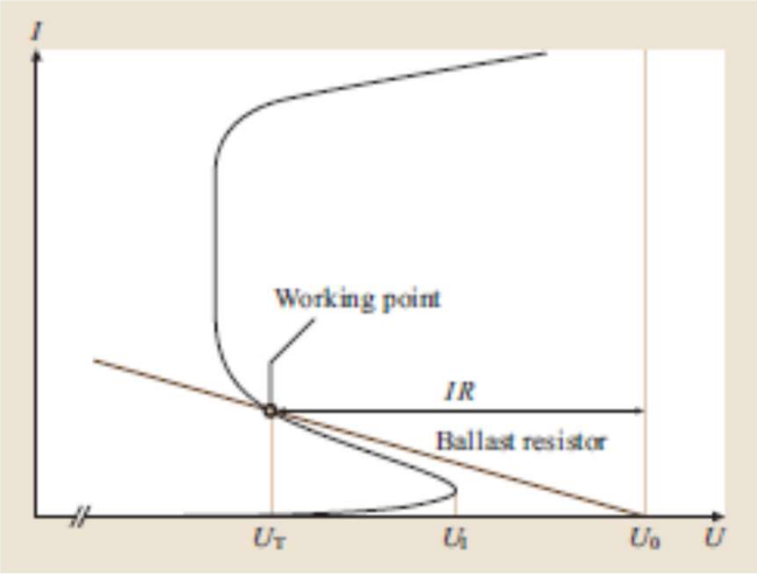

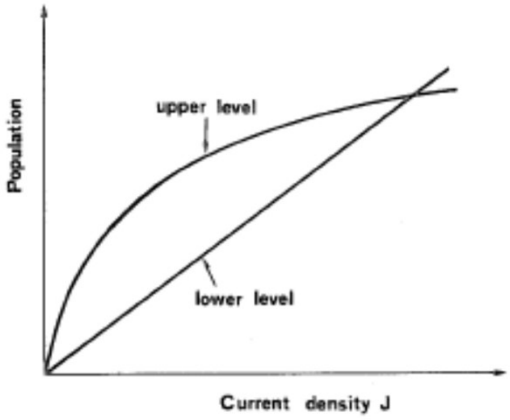

FIG. 10.3. Schematic dependence on current density of upper level and lower level populations in a He-Ne laser.

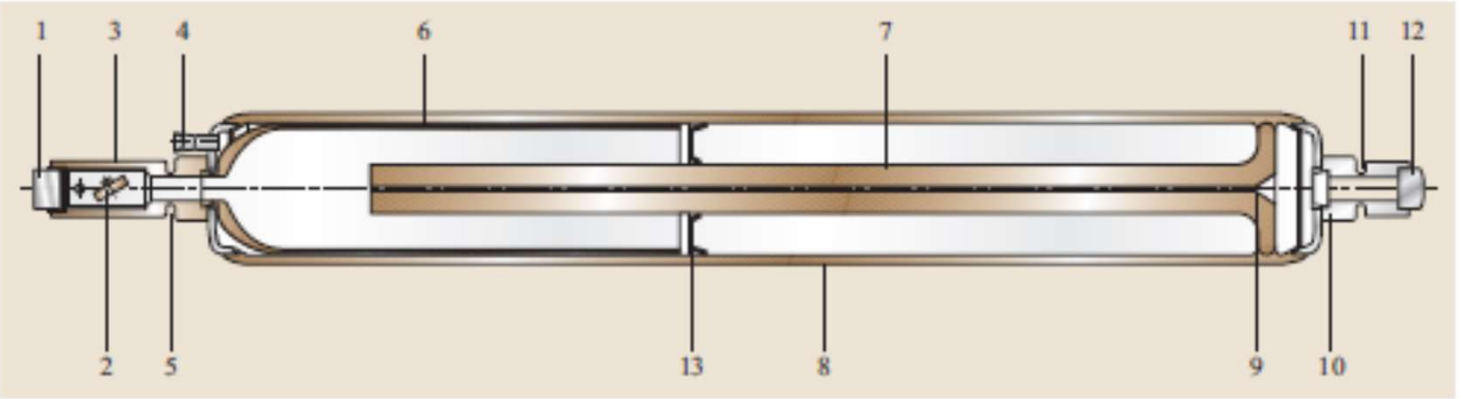

1, 11 zrcadla
3, 10 kovové konce, skleněná trubice 8
6 katoda
7 kapilára
2 někdy Brewster destička
4 výběžek
13 někdy kovová výztuž/pérko
5, 11 zúžení kovu – justování zrcadel

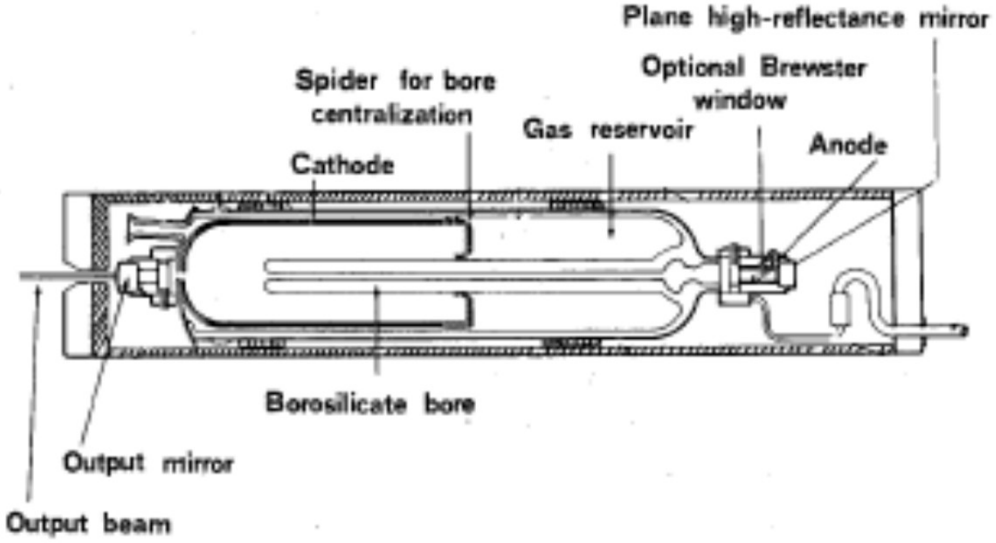

Výkon mW = 0.01 – 0.015 (délka laseru mm) x (průměr kapiláry mm)

Lifetime > 40 000 hod … červený laser

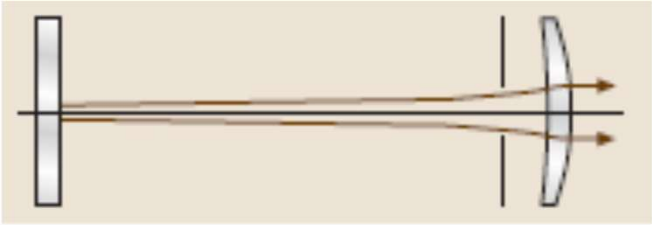

Typický rezonátor

Cu laser

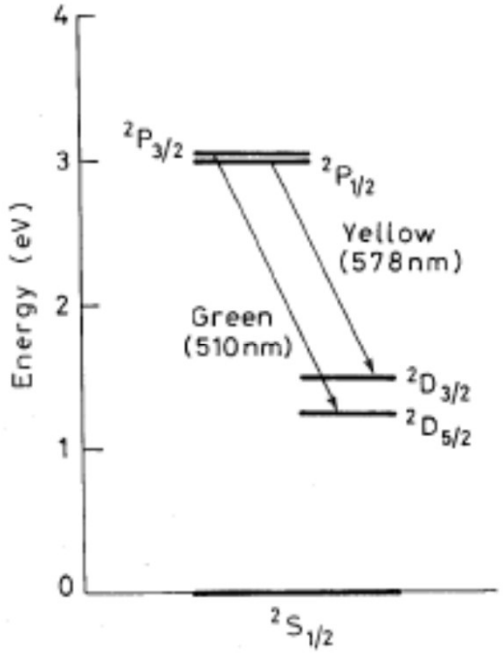

FIG. 10.4. Energy levels of copper atoms relevant to laser operation.

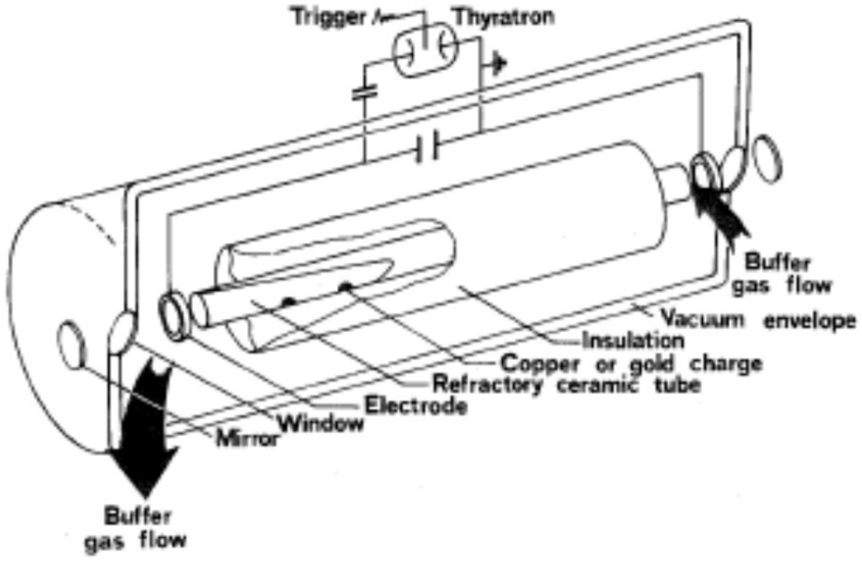

Iontové lasery

10 ns … 4p stavy

0.5 ns
4s stavy

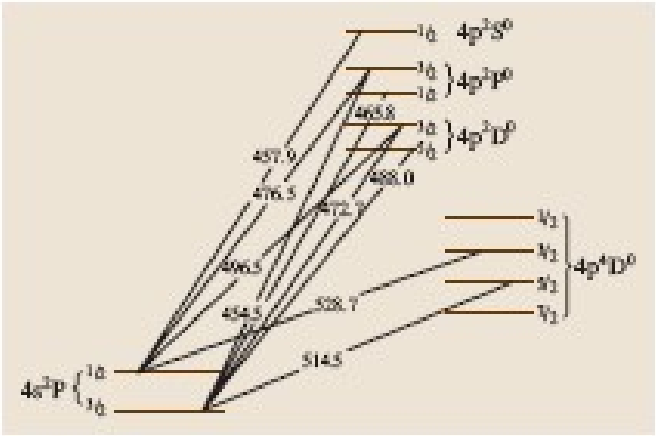

Fig. 11.140 The visible laser transitions of ionized argon (wavelengths in nanometers)

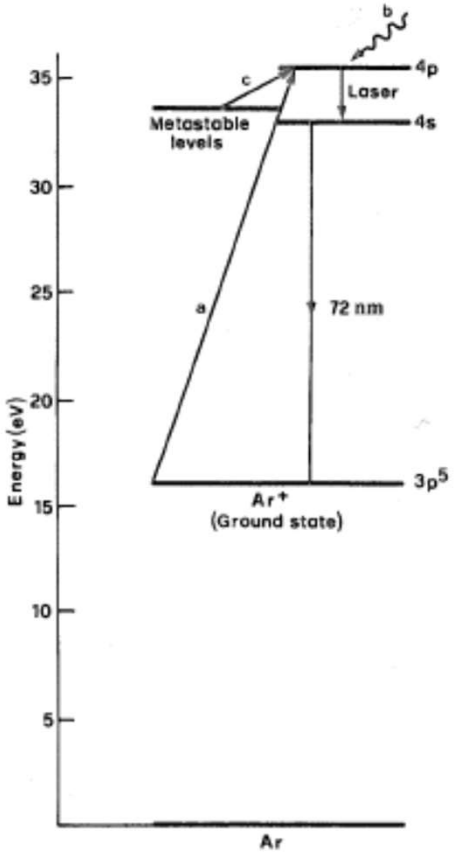

FIG. 10.6. Energy levels of Ar relevant for laser action.

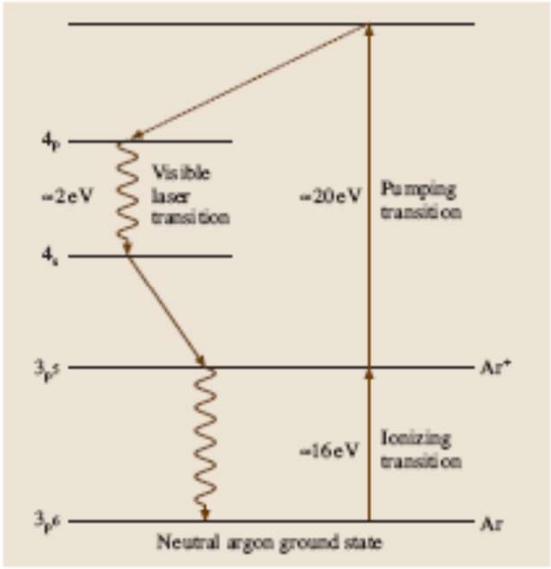

Teplota plasmatu 3000 K

Tlak kolem 1 torr

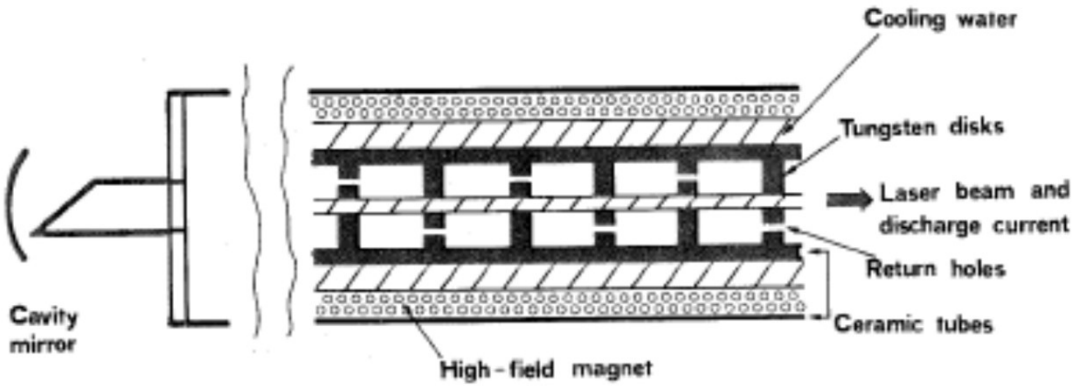
Cooling water
Tungsten disks
Laser beam and discharge current
Return holes
Ceramic tubes
Cavity mirror
High-field magnet

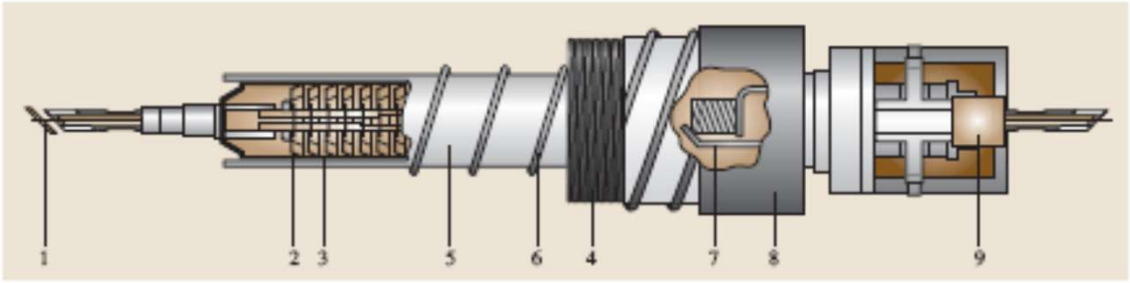
1
2
3
5
6
4
7
8
9

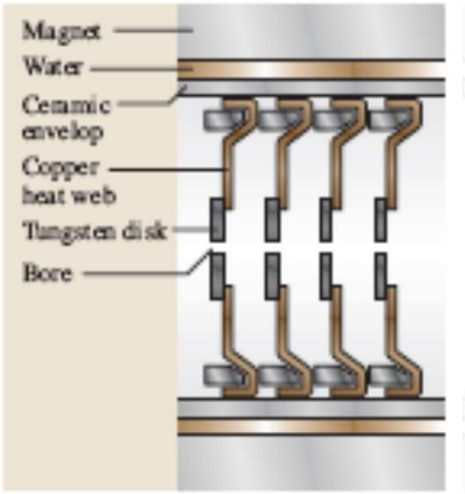
Magnet
Water
Ceramic envelop
Copper heat web
Tungsten disk
Bore

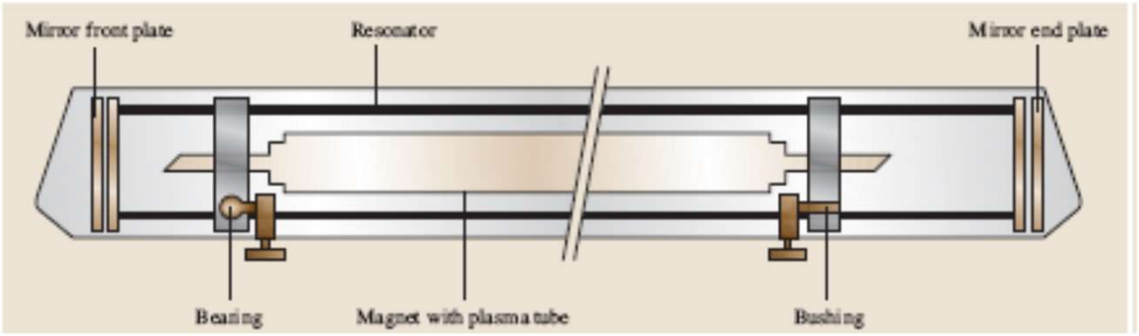
Mirror front plate
Resonator
Mirror end plate
Bearing
Magnet with plasma tube
Bushing

Powers available in a type of laser (W) (not all wavelengths are available simultaneously)					
Available wavelengths (nm)	Lasing species	Large-frame water cooled (W)	Mid-frame water cooled (W)	Large air-cooled (W)	Small air-cooled (W)
275.4	Argon	0.375			
300.3	Argon	0.5			
302.4	Argon	0.5			
305.5	Argon	0.17			
333.6	Argon	0.4			
334.5	Argon	0.8			
335.8	Argon	0.8			
350.7	Krypton	2.0	0.3		
351.1	Argon	1.5	0.18		
351.4	Argon	0.5	0.06		
356.4	Krypton	0.5	0.12		
363.8	Argon	2.0	0.25		
406.7	Krypton	1.2	0.22		
413.1	Krypton	2.5	0.3		
415.4	Krypton	0.35			
454.5	Argon	0.8	0.18	0.005	0.002
457.9	Argon	1.5	0.55	0.015	0.005
465.8	Argon	0.8	0.24	0.015	0.005
468.0	Krypton	0.5	0.1		
472.7	Argon	1.3	0.32		
476.2	Krypton	0.4	0.1		
476.5	Argon	3.0	1.0	0.025	0.008
482.5	Krypton	0.4	0.05		
488.0	Argon	8.0	2.5	0.1	0.03
496.5	Argon	3.0	1.0	0.03	0.012
501.7	Argon	1.8	0.64	0.015	0.005
514.5	Argon	10.0	3.2	0.1	0.025
528.7	Argon	1.8	0.55	0.01	
530.9	Krypton	1.5	0.25		
568.2	Krypton	0.6	0.25	0.02	
631.2	Krypton	0.2			
647.1	Krypton	3.0	0.8	0.015	
676.4	Krypton	0.9	0.15		
752.5	Krypton	1.2	0.15		
793.1	Krypton	0.1			
799.3	Krypton	0.2	0.03		

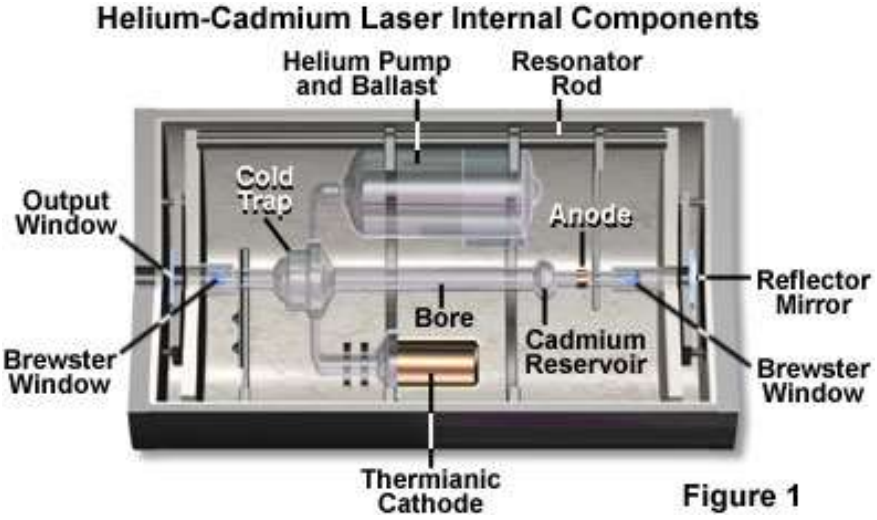

Figure 1

325 nm, 442 nm

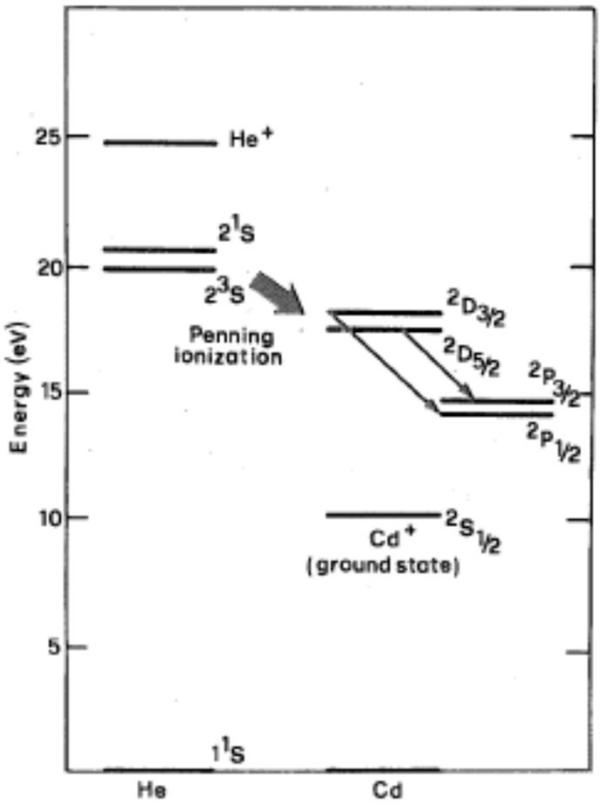

FIG. 10.8. Relevant energy levels in the He-Cd laser.

$$A^* + B \rightarrow A + B^+ + e$$

TABLE 10.1. Spectroscopic properties of laser transitions and gas mixture composition in some relevant atomic and ionic gas lasers

Laser Type	He-Ne	Copper Vapor	Argon Ion	He-Cd
Laser wavelength (nm)	633	510.5	514.5	441.6
Cross section (10^{-14} cm^2)	30	9	25	9
Upper state lifetime (ns)	150	500	6	700
Lower state lifetime (ns)	10	$\approx 10^4$	$\sim$1	1
Transition linewidth (GHz)	1.5	2.5	3.5	1
Partial pressures of gas mixture (Torr)	4 (He) 0.8 (Ne)	40 (He) 0.1-1 (Cu)	0.1 (Ar)	10 (He) 0.1 (Cd)

CO_2 laser …. 10 mikronů

CO laser …… 5 mikronů

Velké výkony, účinnost desítky procent

průmysl

Až cca 10 kW cw

CO_2 laser

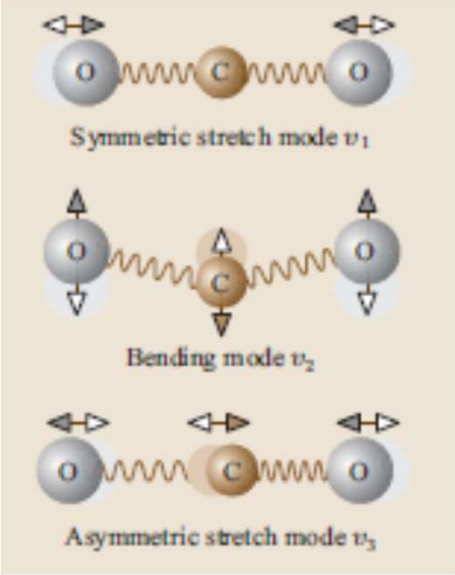

f1 40.51 THZ

f2 20.15 THZ

f3 71.84 THZ

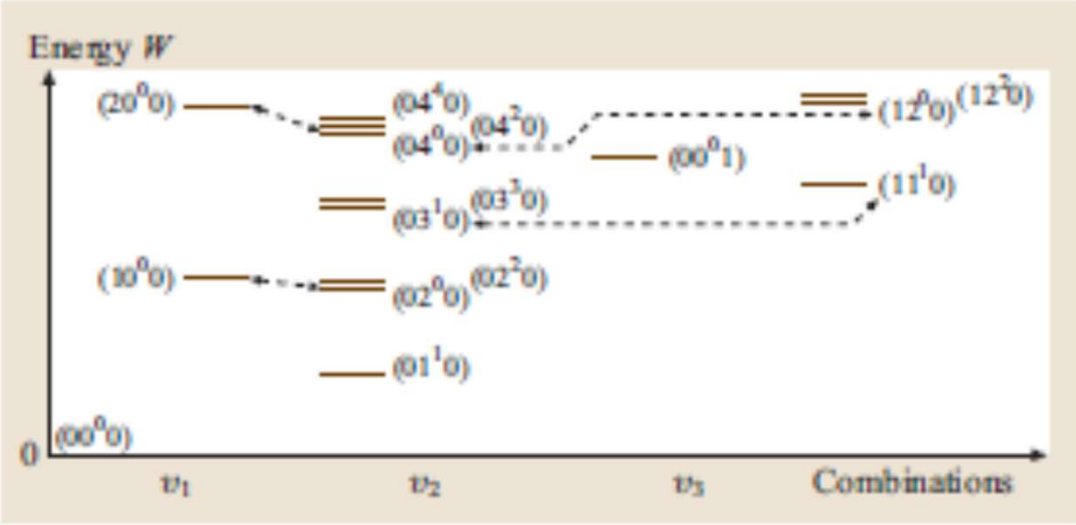

State			Frequency and energy		
Herzberg	AFGL	Type	ϑ (cm^{-1})	f (THz)	W (meV)
(00^00)	00001	Σ_g^+	0	0	0
(01^10)	01101	Π_u	667.380	20.008	82.745
(02^00)	10002	Σ_g^+	1285.408	38.536	159.370
(02^20)	02201	Δ_g	1335.132	40.026	165.535
(10^00)	10001	Σ_g^+	1388.184	41.617	172.113
(03^10)	11102	Π_u	1932.470	57.934	239.596
(03^30)	03301	Φ_u	2003.246	60.056	248.371
(11^10)	11101	Π_u	2076.856	62.263	257.497
(00^01)	00011	Σ_u^+	2349.143	70.426	291.257

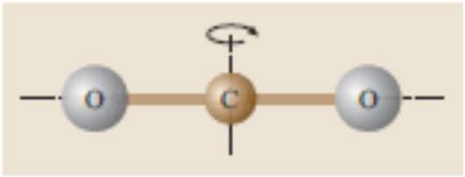
O
C
O

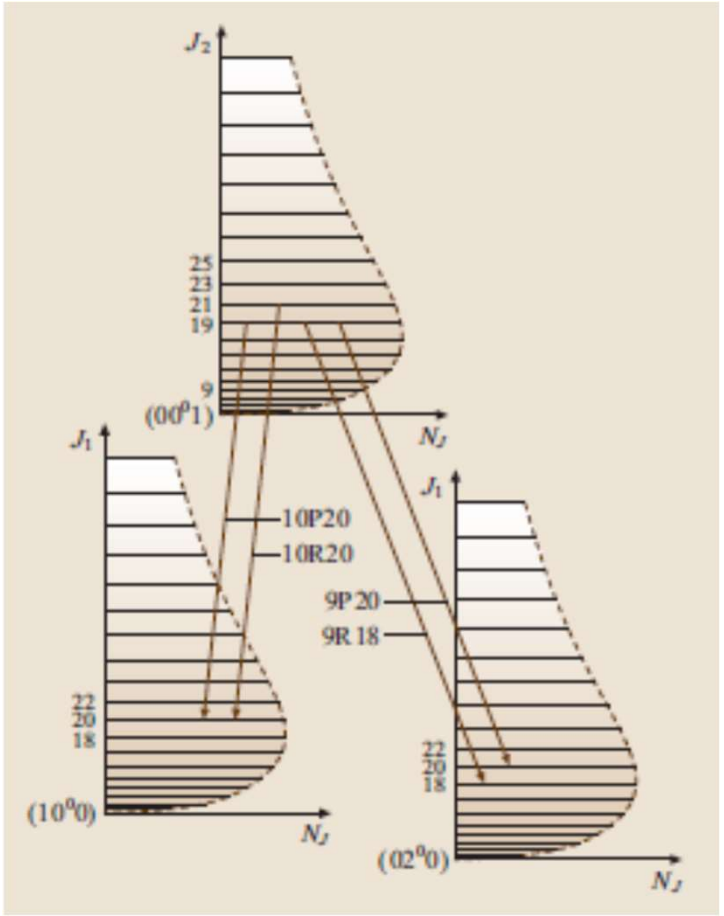
J_2
25
23
21
19
9
$(00^0 1)$
N_J
J_1
10P20
10R20
9P 20
9R 18
22
20
18
$(10^0 0)$
N_J
J_1
22
20
18
$(02^0 0)$
N_J

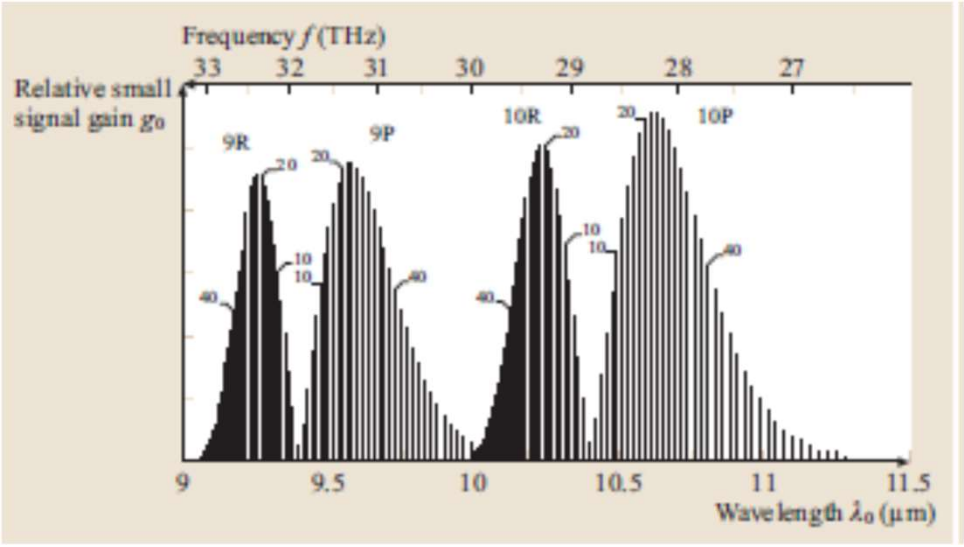
Frequency f (THz)
33
32
31
30
29
28
27
Relative small signal gain g_0
9R
9P
10R
10P
20
40
10
9
9.5
10
10.5
11
11.5
Wavelength λ_0 (μm)

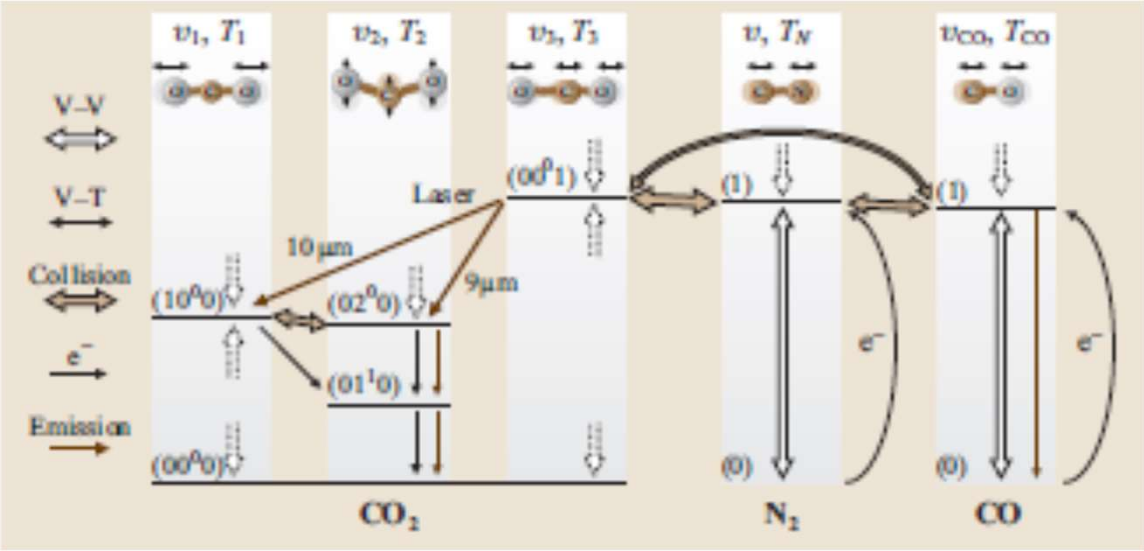

Přenos excitační energie: N_2

Směs CO_2 : N_2 : He 1 : 2 : 8

Chlazení: He

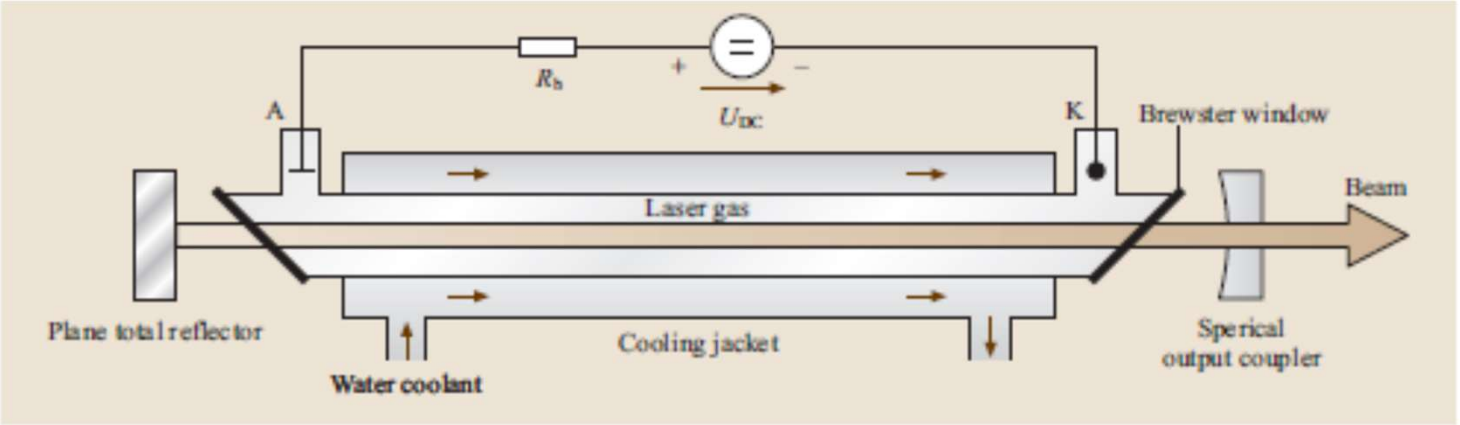
R_b
+
−
U_{DC}
A
K
Brewster window
Beam
Laser gas
Plane total reflector
Cooling jacket
Sperical
output coupler
Water coolant

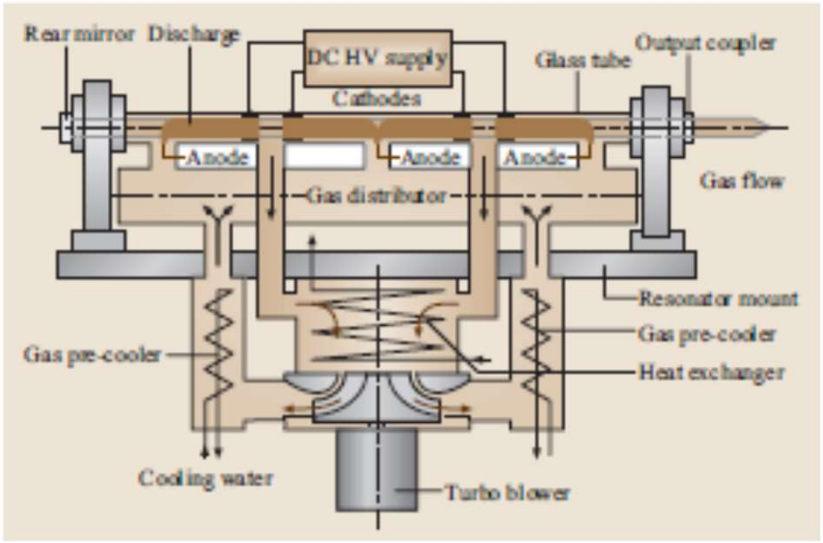
Rear mirror
Discharge
DC HV supply
Glass tube
Output coupler
Cathodes
Anode
Anode
Anode
Gas flow
Gas distributor
Resonator mount
Gas pre-cooler
Gas pre-cooler
Heat exchanger
Cooling water
Turbo blower

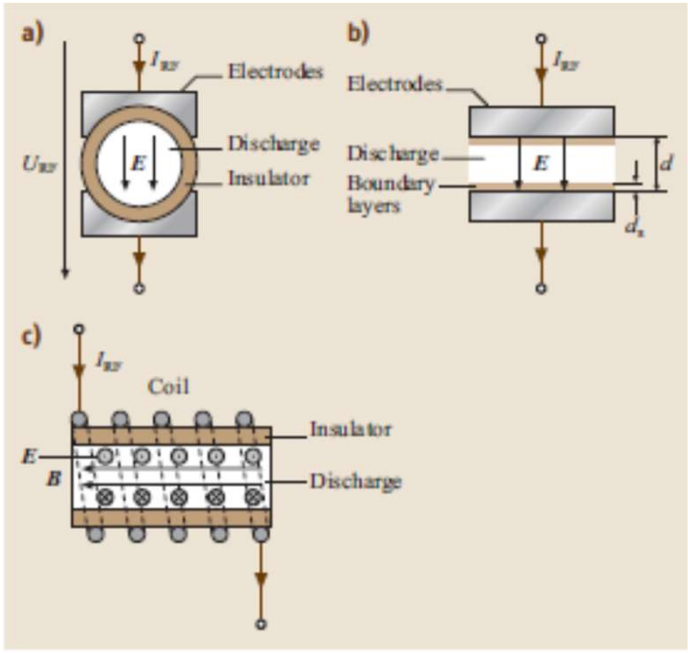
a)
I_{RF}
Electrodes
U_{RF}
Discharge
E
Insulator
b)
I_{RF}
Electrodes
Discharge
E
d
Boundary
layers
d_s
c)
I_{RF}
Coil
Insulator
E
B
Discharge

DC

RF

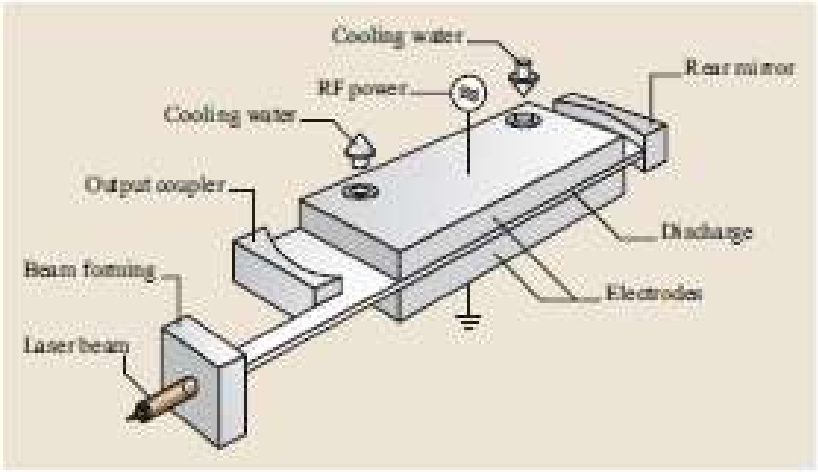

RF, waveguide

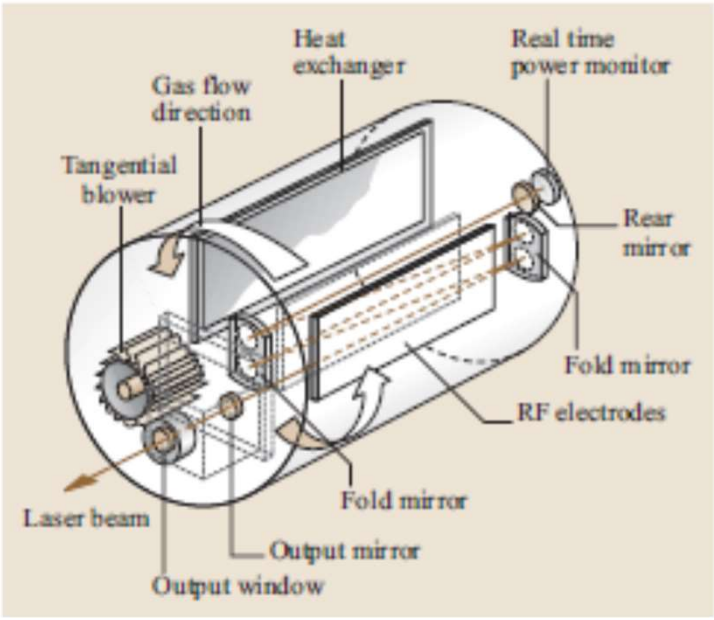

RF, TEA

Excimerové lasery

Excited dimer,

Excimerové lasery … exiplexy

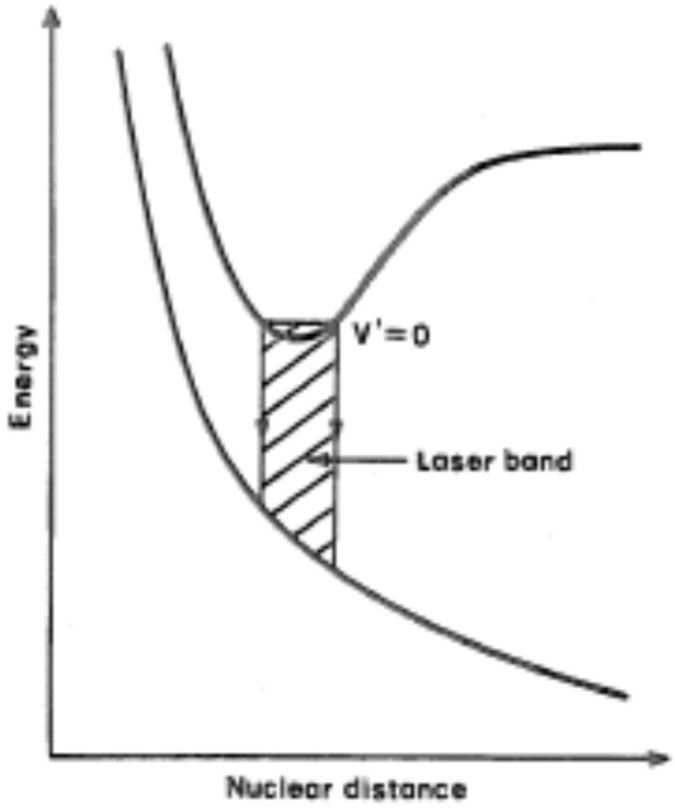

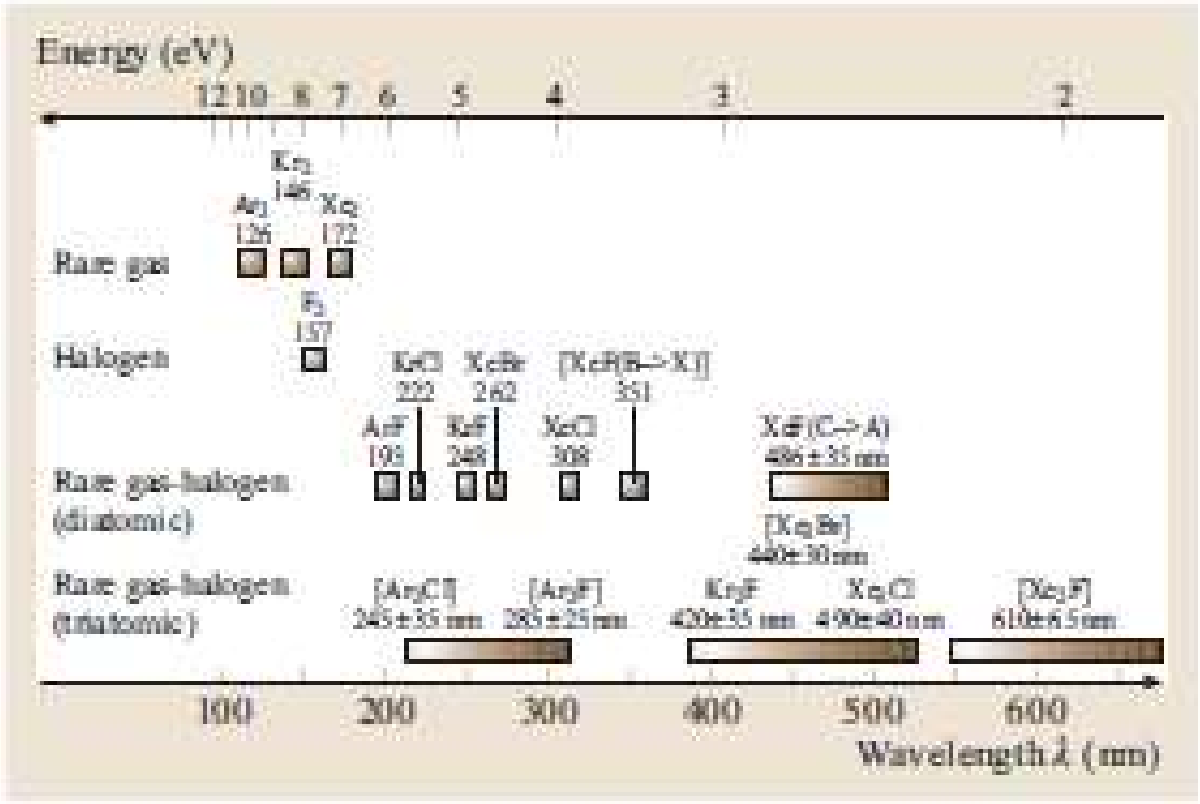

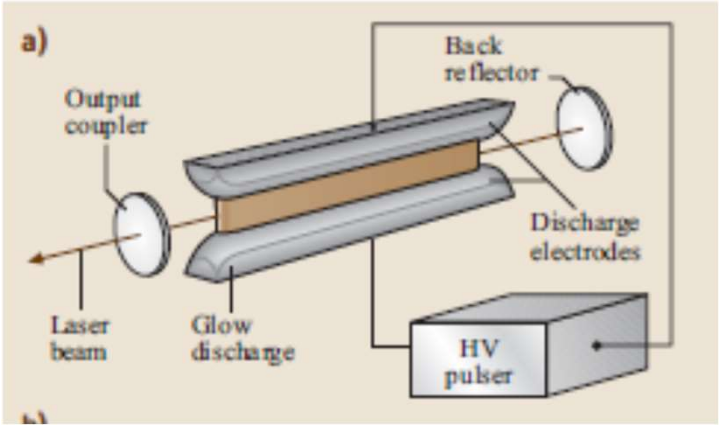

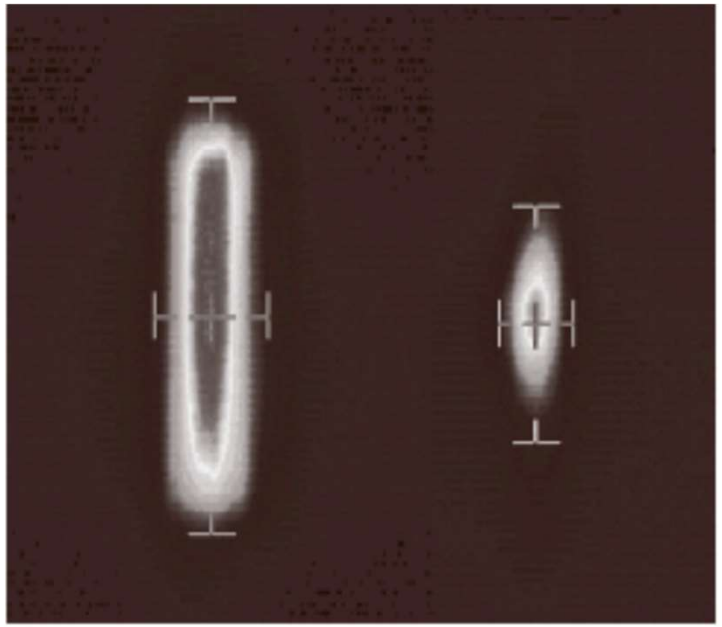

Fig. 11.166 Near-field (*left*) and far-field profile (*right*) of F_2 laser (157 nm, Novaline F1030, Lambda Physik) recorded simultaneously with a camera-based measurement system. The evaluated second-moment beam widths in the horizontal and vertical directions are also indicated

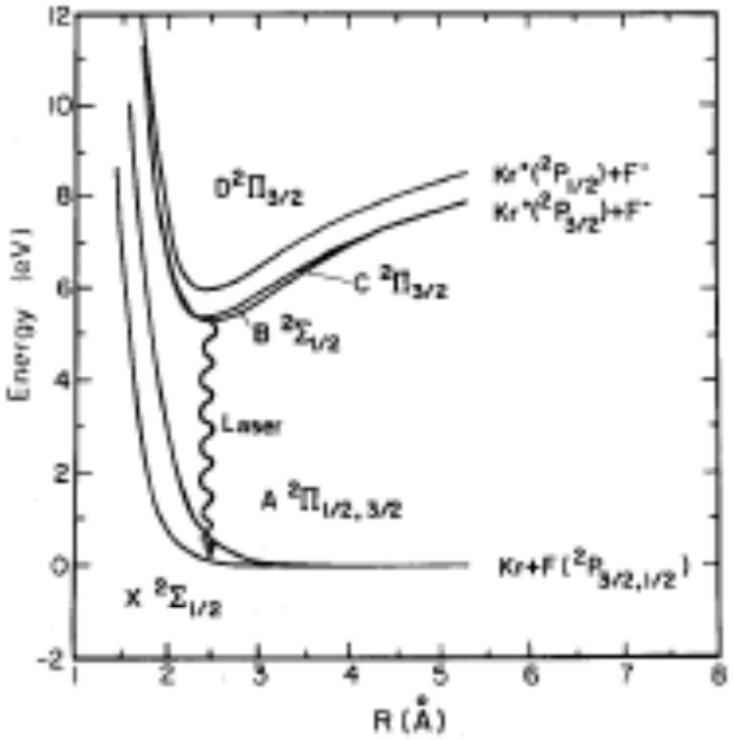

$$e + \mathrm{Kr} \rightarrow e + \mathrm{Kr}^*$$

$$\mathrm{Kr}^* + \mathrm{F_2} \rightarrow (\mathrm{KrF})^* + \mathrm{F}$$

$$e + \mathrm{Kr} \rightarrow 2e + \mathrm{Kr}^+$$

$$e + \mathrm{F_2} \rightarrow \mathrm{F}^- + \mathrm{F}$$

$$\mathrm{F}^- + \mathrm{Kr}^+ + \mathrm{M} \rightarrow (\mathrm{KrF})^* + \mathrm{M}$$

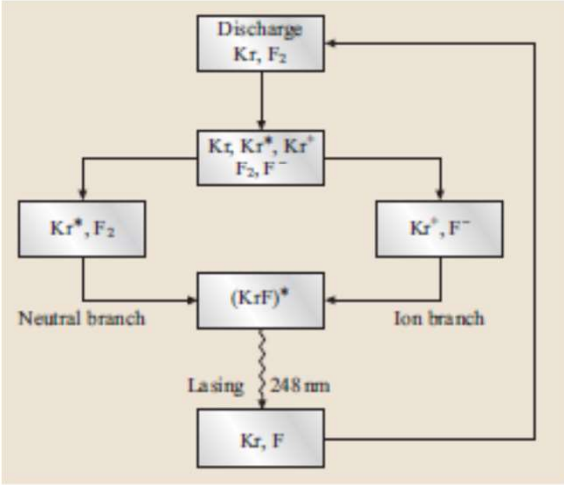

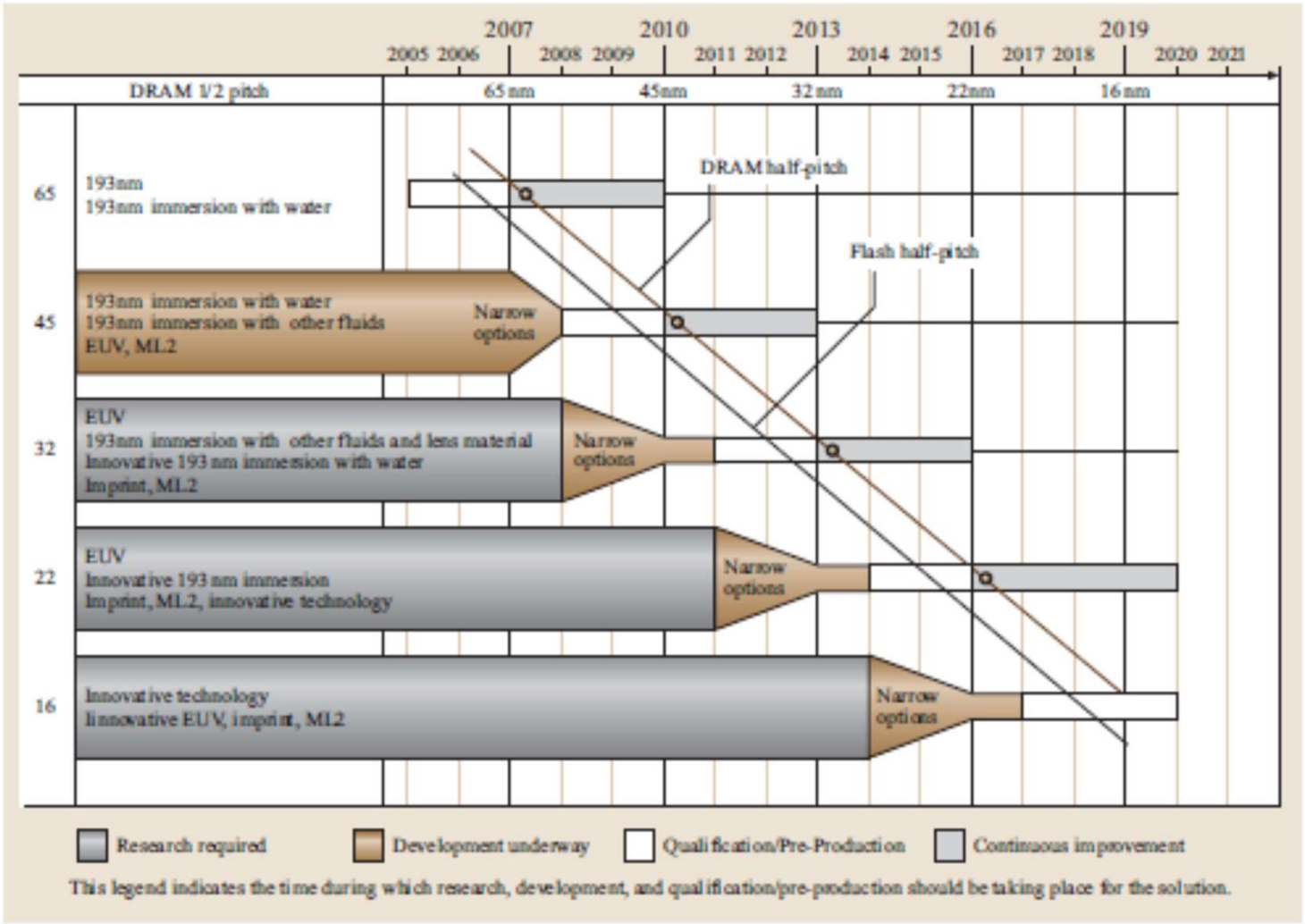

Fig. 11.168 Potential lithography exposure tool solutions according to the *International Technology Roadmap for Semiconductors 2005* [11.1505]. Courtesy ITRS

Chemické lasery

$$F + H_2 \rightarrow HF^* + H$$

$$H + F_2 \rightarrow HF^* + F$$

$$\lambda = 2.7\text{–}3.3\ \mu m$$

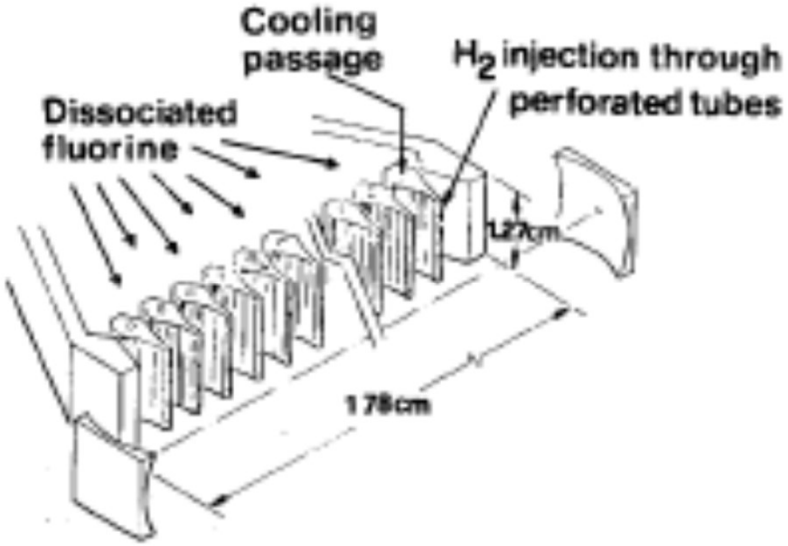

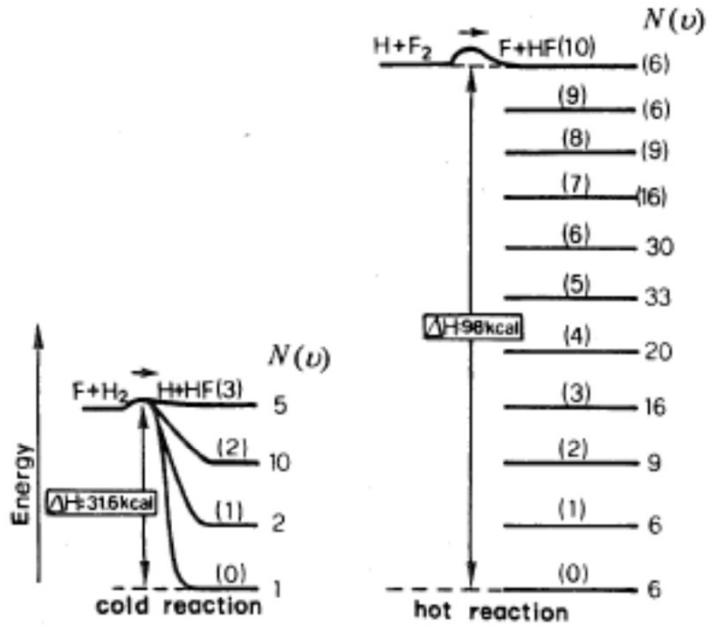

FIG. 10.22. Pumping vibrational levels of the HF molecule by the two reactions (a) $F + H_2 \rightarrow HF^* + H$ and (b) $H + F_2 \rightarrow HF^* + F$. The relative populations $N(v)$ of each vibrational state of quantum number v are also indicated in the two figures.

Plynový dynamický laser

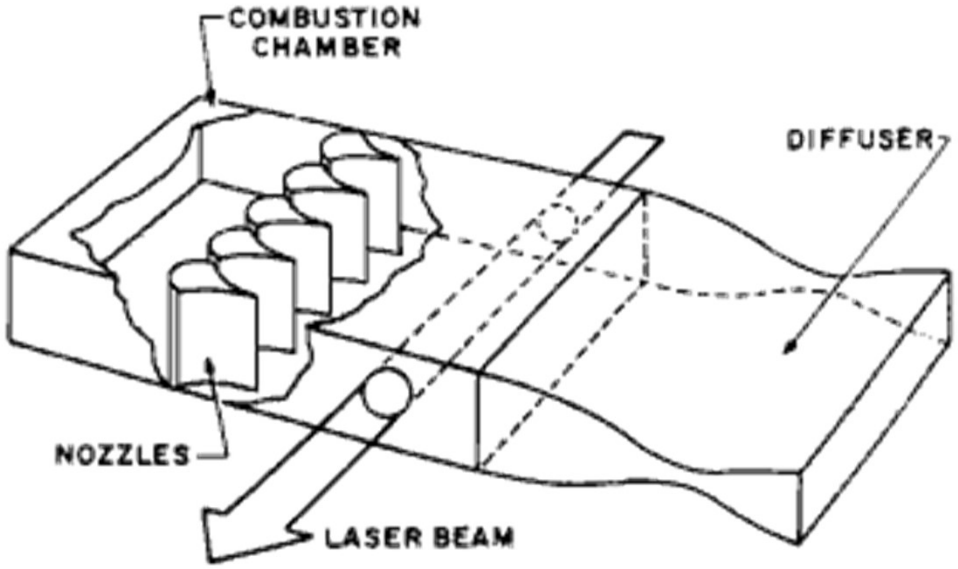

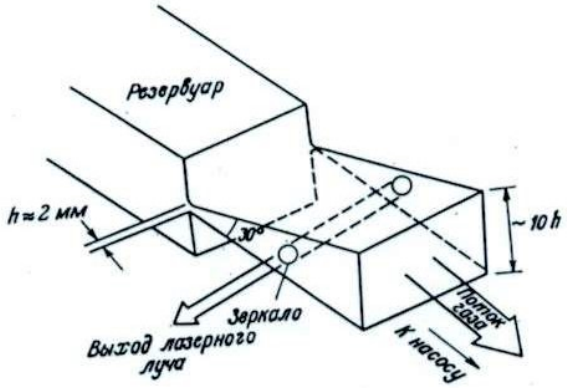

. Схема газодинамического лазера.

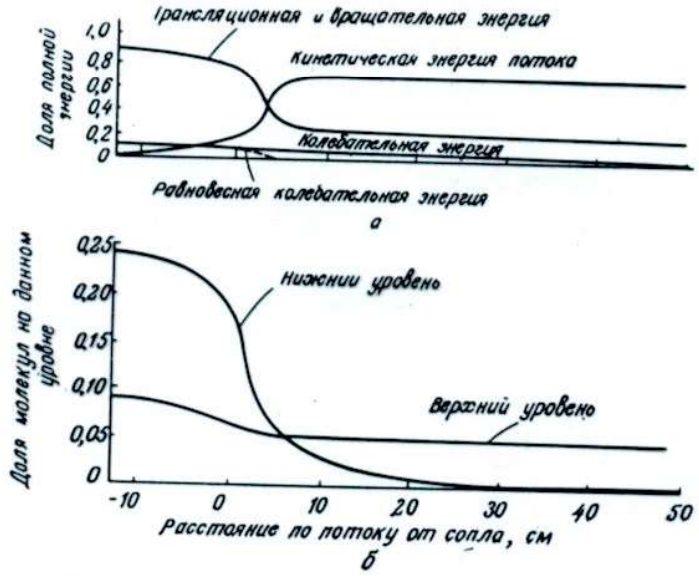

Механизм возникновения инверсии населенностей в газодинамическом лазере [7].

а — зависимость доли полной энергии, приходящейся на различные степени свободы, от расстояния от сопла; б — зависимость доли молекул CO_2 на нижнем и верхнем лазерных уровнях от расстояния в направлении потока из сопла.

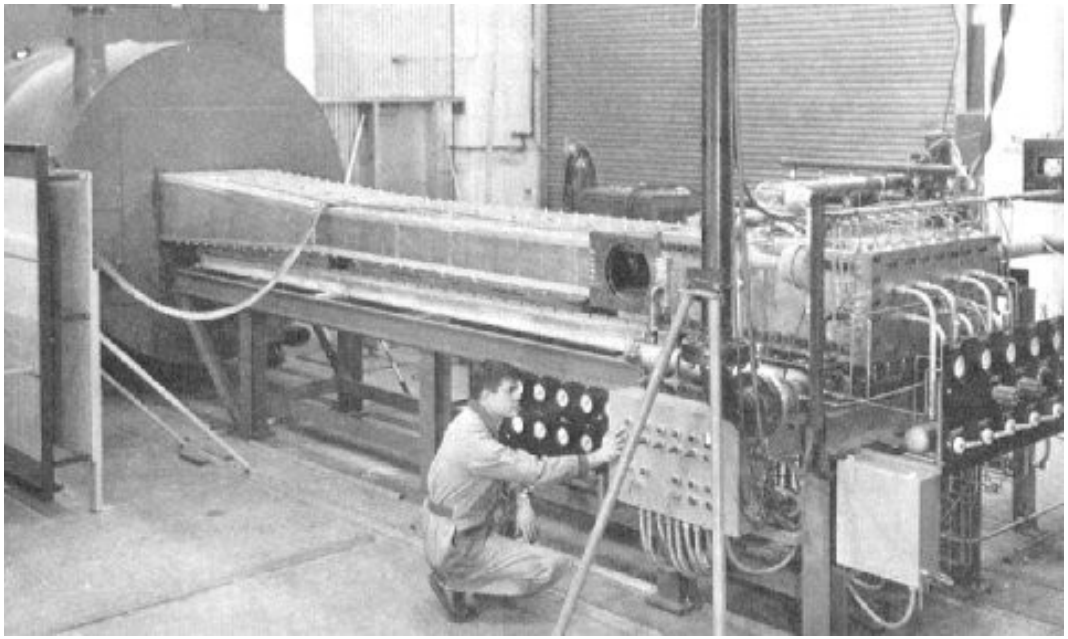

Large scale 135 Kilowatt gasdynamic laser at Avco Everett Research Lab, Inc. was among the first very high power lasers.

Barvivové lasery

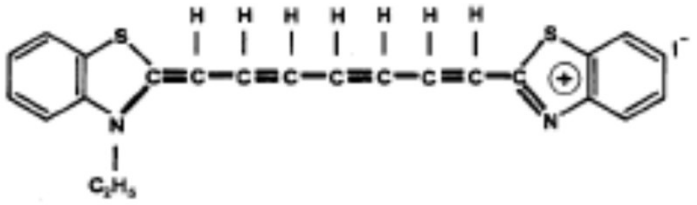

(a)

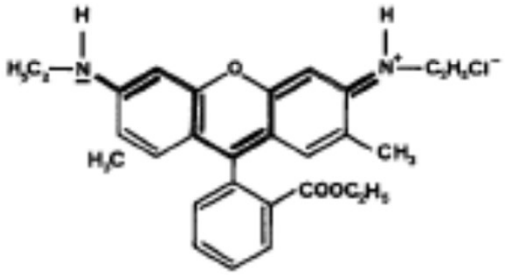

(b)

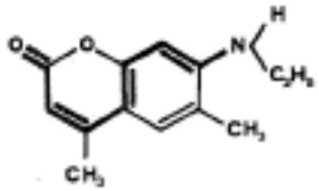

(c)

FIG. 9.12. Chemical structure of some common dyes: (a) 3,3′ diethyl thiatricarbocyanine iodide, (b) rhodamine 6G, and (c) coumarin 2. In each case the chromophoric region of the dye is indicated by heavier lines.

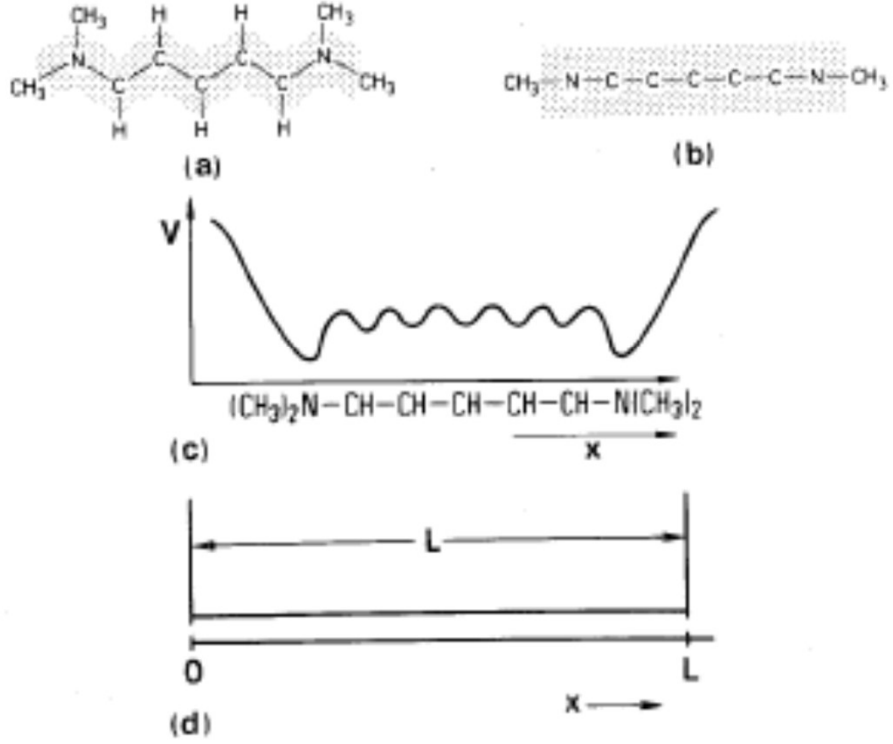
(a)
(b)
V
$(CH_3)_2N-CH-CH-CH-CH-CH-N(CH_3)_2$
x
(c)
L
0
L
x
(d)

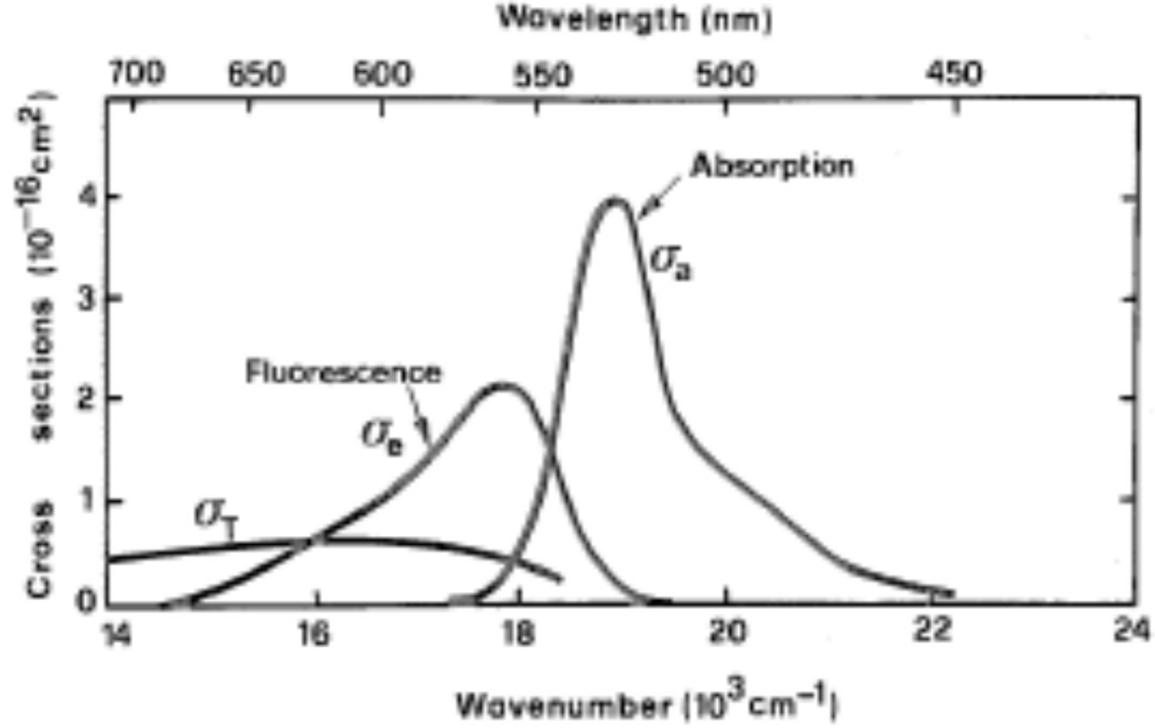
Wavelength (nm)
700
650
600
550
500
450
Cross sections (10^{-16}cm^2)
0
1
2
3
4
Absorption
σ_a
Fluorescence
σ_e
σ_T
14
16
18
20
22
24
Wavenumber (10^3cm^{-1})

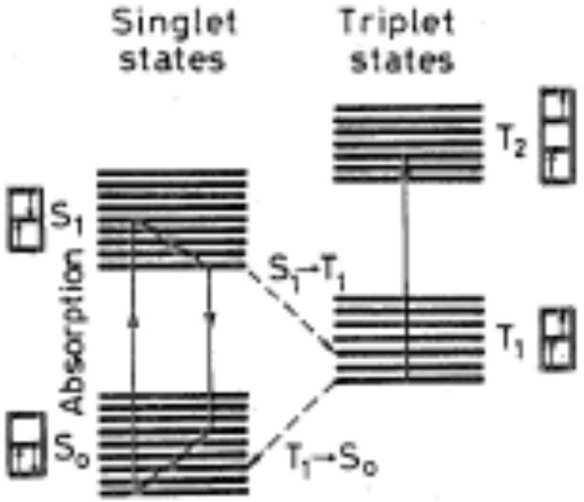
Singlet states
Triplet states
S_1
T_2
T_1
S_0
Absorption
$S_1 \rightarrow T_1$
$T_1 \rightarrow S_0$

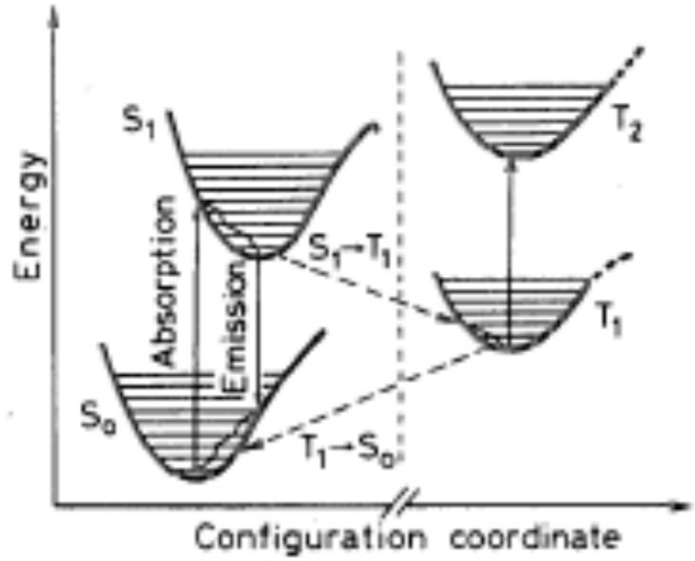
Energy
S_1
T_2
T_1
S_0
Absorption
Emission
$S_1 \rightarrow T_1$
$T_1 \rightarrow S_0$
Configuration coordinate

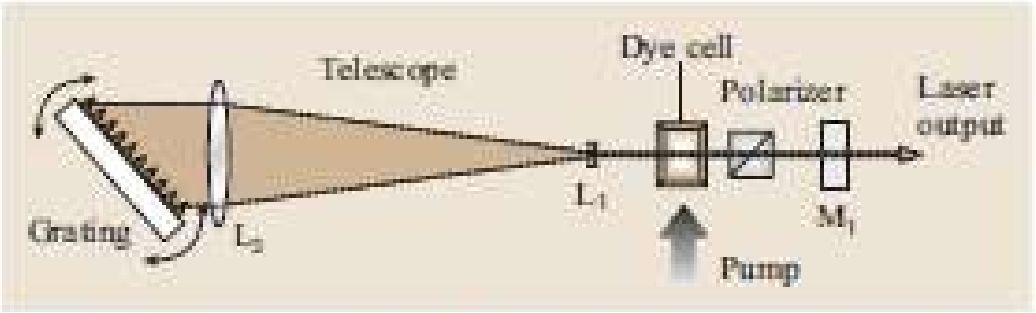

TABLE 9.6. Range of optical and spectroscopic parameters of typical dye laser media

Active Medium Parameter	Values
Wavelengths (nm)	320–1500
Concentration (molar)	10^{-3}–10^{-4}
N_t (10^{19} mol/cm^3)	0.1–1
σ_e (10^{-16} cm^2)	1–4
σ_T (10^{-16} cm^2)	0.5–0.8
$\Delta\lambda$ (nm)	25–50
τ (ns)	2–5
k_{ST}^{-1} (ns)	$\approx$100
τ_T (s)	10^{-7}–10^{-3}
Refractive index	1.3–1.4

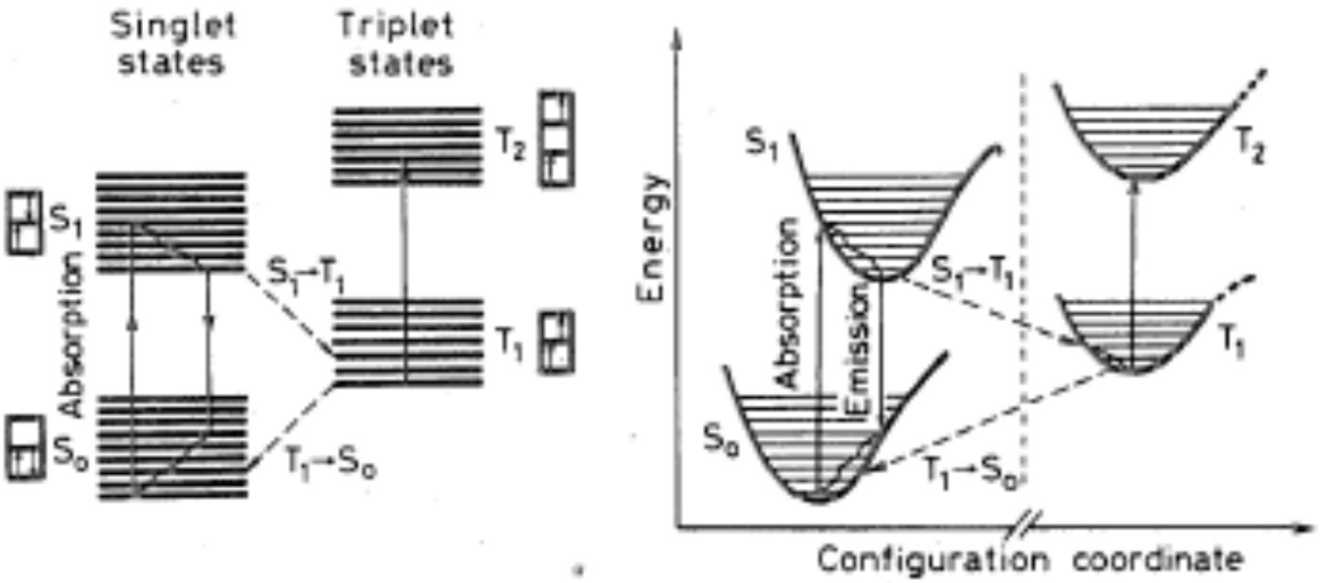

$$\sigma_e N_2 > \sigma_T N_T$$

$$N_T = k_{ST} \tau_T N_2$$

$$\tau_T < \frac{\sigma_e}{\sigma_T k_{ST}}$$

Podmínka cw režimu

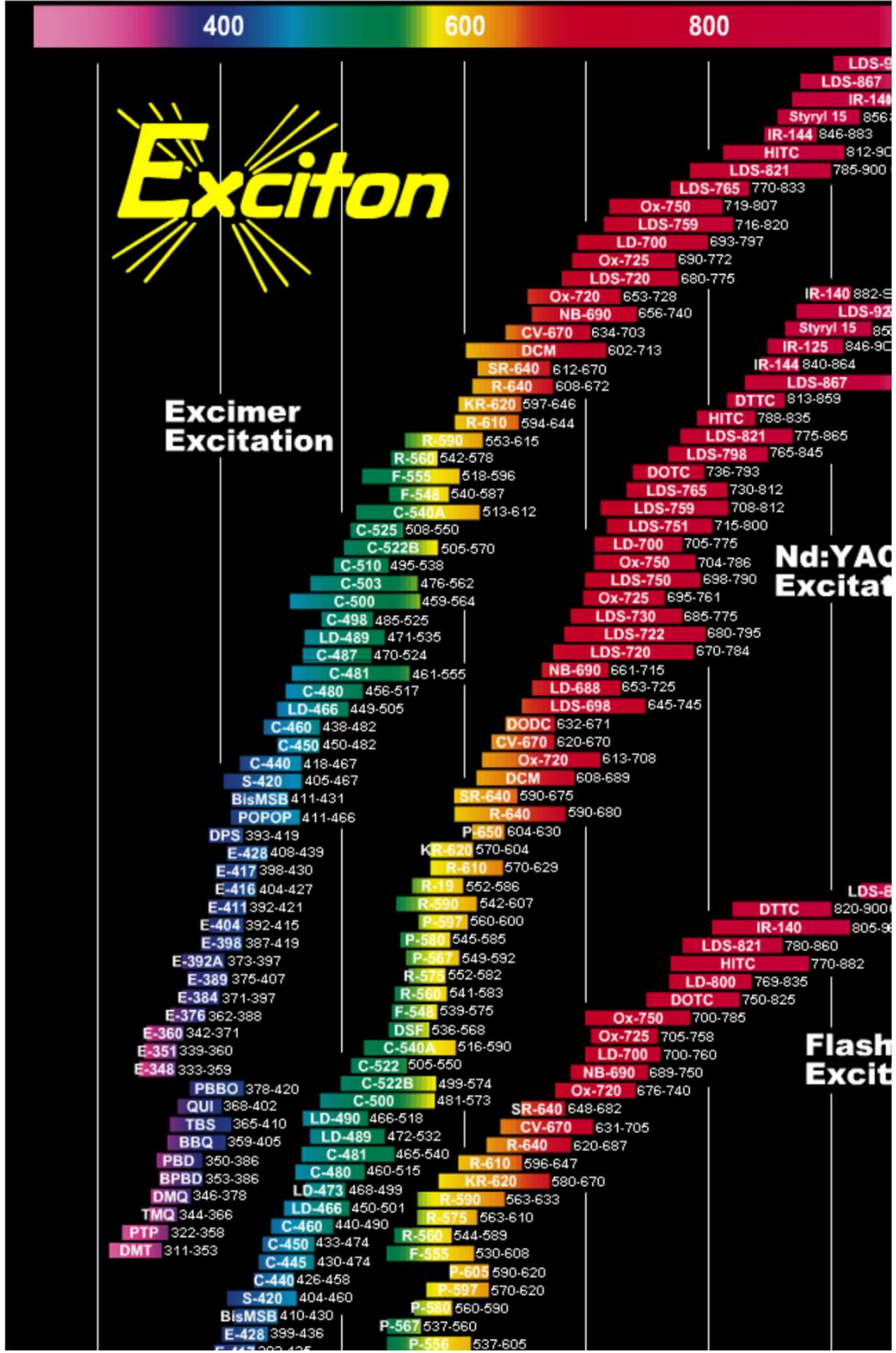
400
600
800
Exciton
Excimer Excitation
Nd:YAG Excitat
Flash Excit
LDS-9
LDS-867
IR-14
Styryl 15 856
IR-144 846-883
HITC 812-90
LDS-821 785-900
LDS-765 770-833
Ox-750 719-807
LDS-759 716-820
LD-700 693-797
Ox-725 690-772
LDS-720 680-775
Ox-720 653-728
NB-690 656-740
CV-670 634-703
DCM 602-713
SR-640 612-670
R-640 608-672
KR-620 597-646
R-610 594-644
R-590 553-615
R-560 542-578
F-555 518-596
F-548 540-587
C-540A 513-612
C-525 508-550
C-522B 505-570
C-510 495-538
C-503 476-562
C-500 459-564
C-498 485-525
LD-489 471-535
C-487 470-524
C-481 461-555
C-480 456-517
LD-466 449-505
C-460 438-482
C-450 450-482
C-440 418-467
S-420 405-467
BisMSB 411-431
POPOP 411-466
DPS 393-419
E-428 408-439
E-417 398-430
E-416 404-427
E-411 392-421
E-404 392-415
E-398 387-419
E-392A 373-397
E-389 375-407
E-384 371-397
E-376 362-388
E-360 342-371
E-351 339-360
E-348 333-359
PBBO 378-420
QUI 368-402
TBS 365-410
BBQ 359-405
PBD 350-386
BPBD 353-386
DMQ 346-378
TMQ 344-366
PTP 322-358
DMT 311-353
IR-140 882-9
LDS-92
Styryl 15 85
IR-125 846-9
IR-144 840-864
LDS-867
DTTC 813-859
HITC 788-835
LDS-821 775-865
LDS-798 765-845
DOTC 736-793
LDS-765 730-812
LDS-759 708-812
LDS-751 715-800
LD-700 705-775
Ox-750 704-786
LDS-750 698-790
Ox-725 695-761
LDS-730 685-775
LDS-722 680-795
LDS-720 670-784
NB-690 661-715
LD-688 653-725
LDS-698 645-745
DODC 632-671
CV-670 620-670
Ox-720 613-708
DCM 608-689
SR-640 590-675
R-640 590-680
P-650 604-630
KR-620 570-604
R-610 570-629
R-19 552-586
R-590 542-607
P-597 560-600
P-580 545-585
P-567 549-592
R-575 552-582
R-560 541-583
F-548 539-575
DSF 536-568
C-540A 516-590
C-522 505-550
C-522B 499-574
C-500 481-573
LD-490 466-518
LD-489 472-532
C-481 465-540
C-480 460-515
LD-473 468-499
LD-466 450-501
C-460 440-490
C-450 433-474
C-445 430-474
C-440 426-458
S-420 404-460
BisMSB 410-430
E-428 399-436
LDS-8
DTTC 820-900
IR-140 805-9
LDS-821 780-860
HITC 770-882
LD-800 769-835
DOTC 750-825
Ox-750 700-785
Ox-725 705-758
LD-700 700-760
NB-690 689-750
Ox-720 676-740
SR-640 648-682
CV-670 631-705
R-640 620-687
R-610 596-647
KR-620 580-670
R-590 563-633
R-575 563-610
R-560 544-589
F-555 530-608
P-605 590-620
P-597 570-620
P-580 560-590
P-567 537-560
P-556 537-605

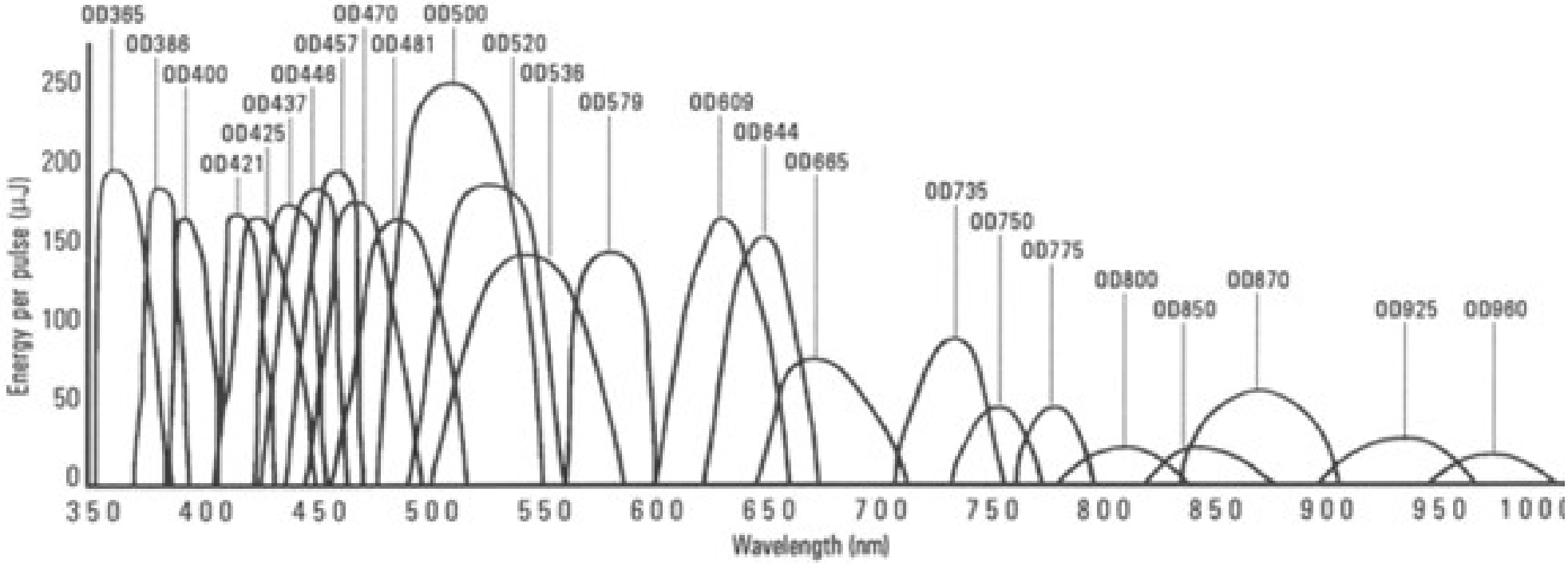

NITROGEN PUMPED DYES (LASER SCIENCE,INC)

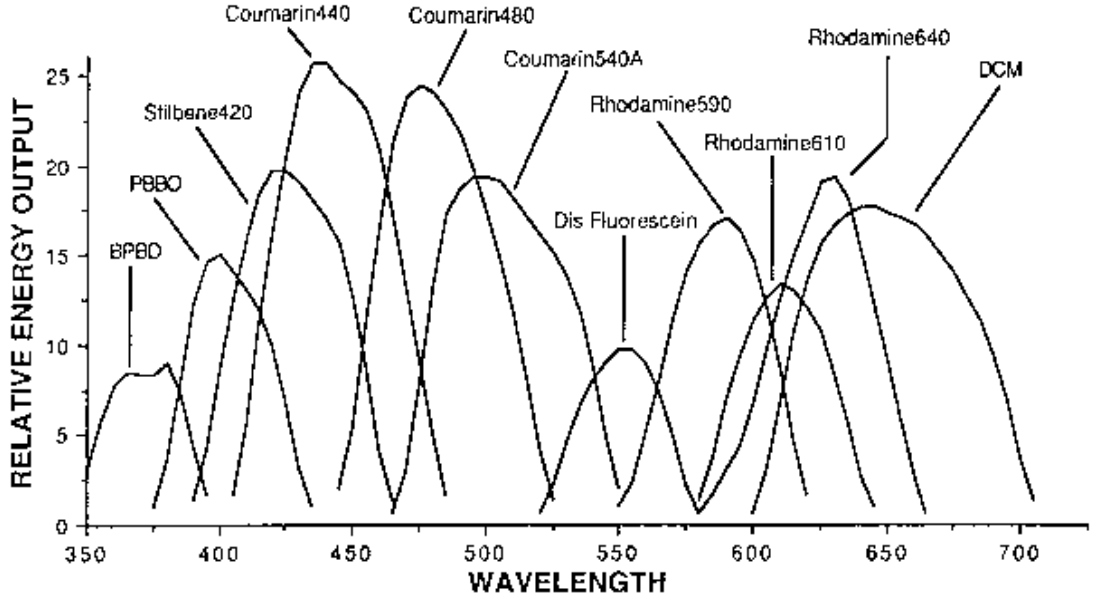

Pevnolátkové lasery

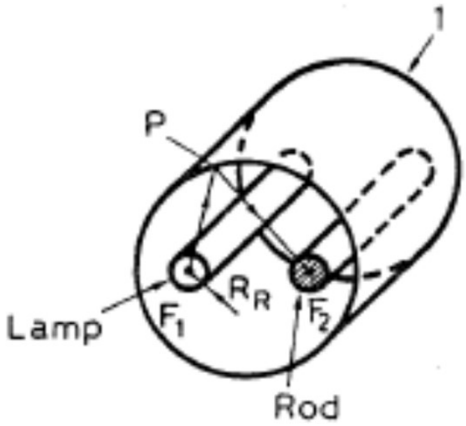
1
P
Lamp
F1
RR
F2
Rod


1
Lamp
Rod

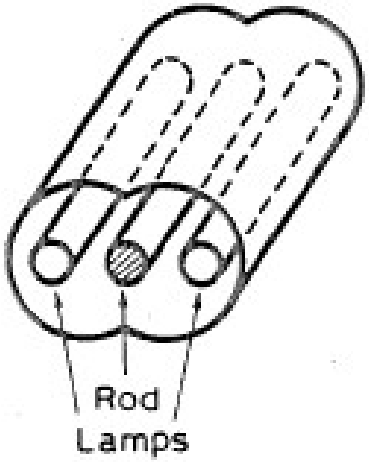
Rod
Lamps

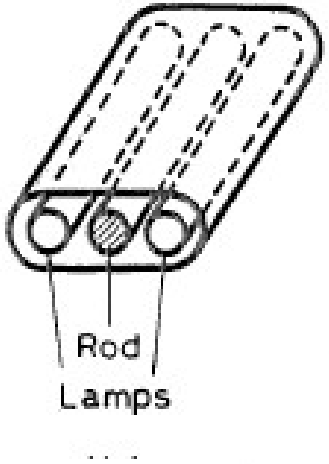
Rod
Lamps

čerpání

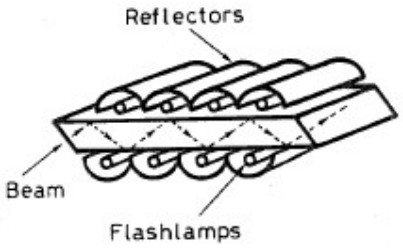
Reflectors
Beam
Flashlamps

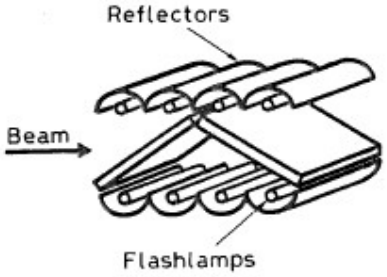
Reflectors
Beam
Flashlamps

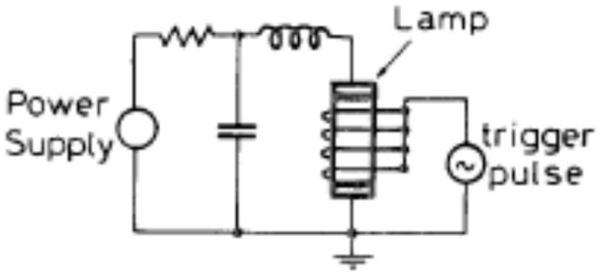
Lamp
Power
Supply
trigger
pulse

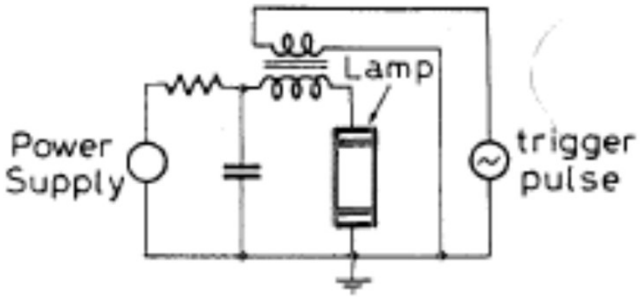
Lamp
Power
Supply
trigger
pulse

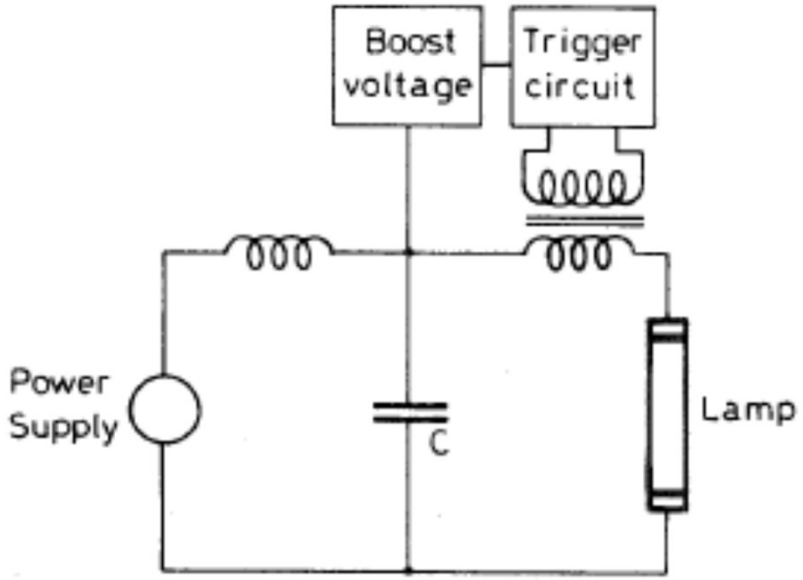
Boost
voltage
Trigger
circuit
Power
Supply
C
Lamp

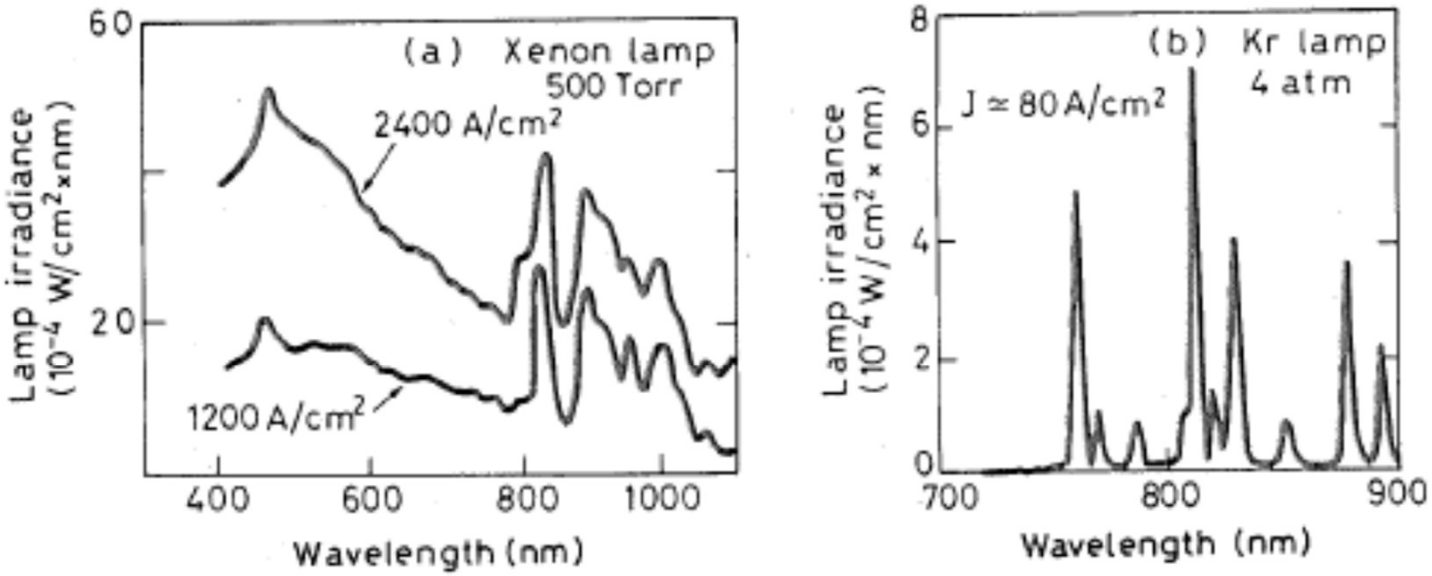

FIG. 6.6. Comparison of the emission spectra of an (a) Xe flashlamp at 500-Torr pressure and of a (b) cw-pumped Kr arc lamp at 4-atm pressure.

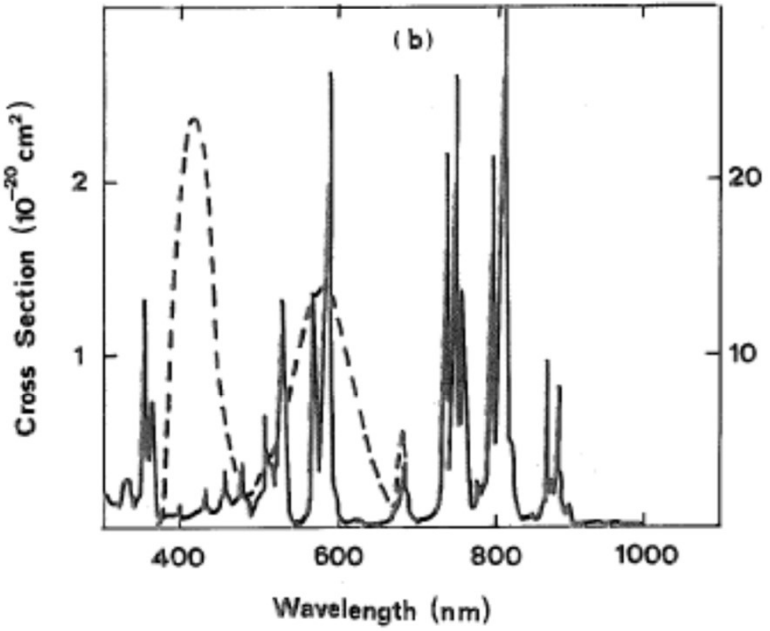

FIG. 6.7. Absorption cross section of Nd^{3+} ion in YAG (*solid line*) and of a Cr^{3+} ion in alexandrite (*dashed line*). The left-hand scale refers to the cross section of Nd:YAG and the right-hand scale to alexandrite. For alexandrite the average of the three values measured for polarization parallel to the *a*-, *b*-, and *c*-axes has been taken.

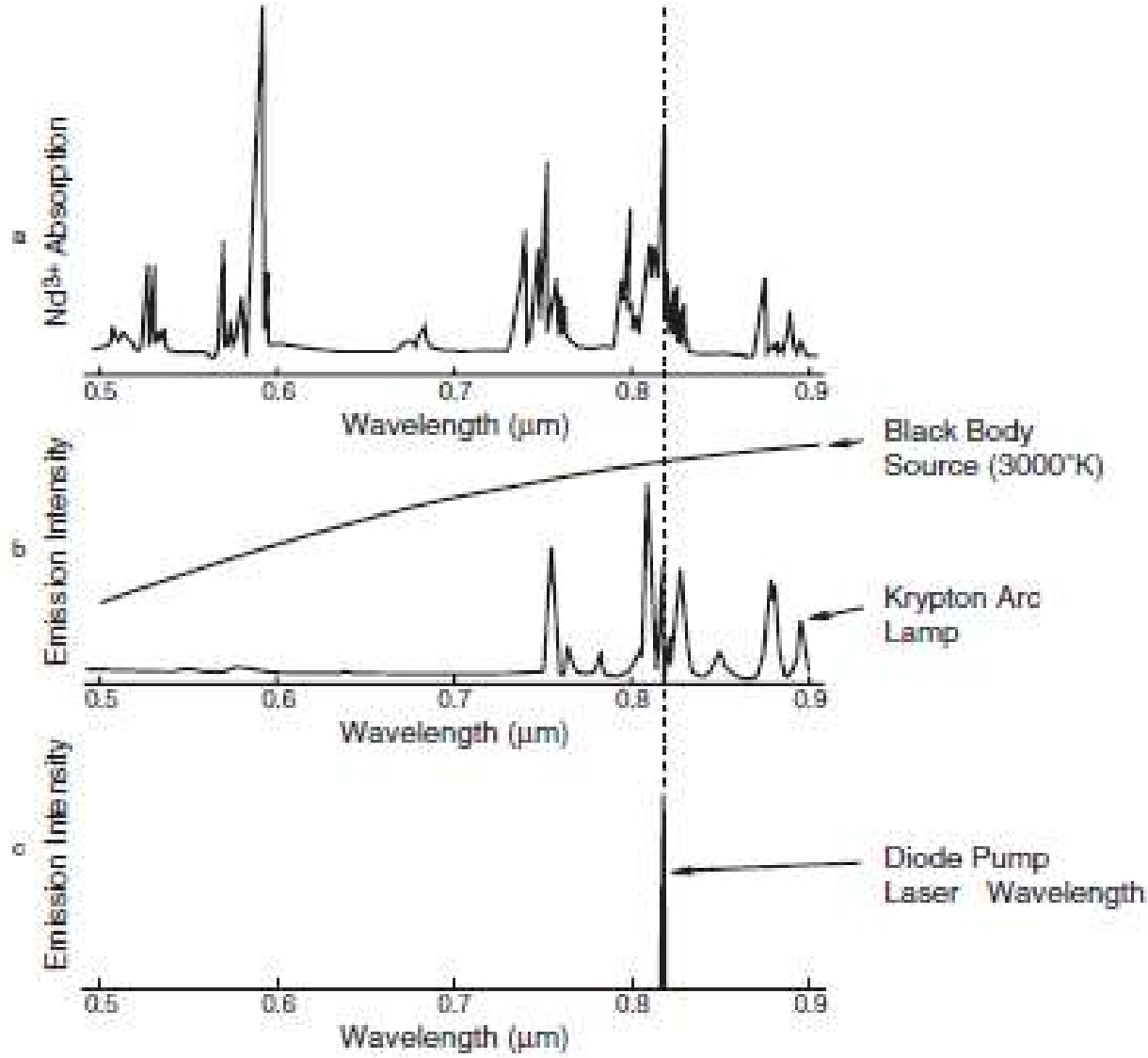
a
Nd3+ Absorption
0.5
0.6
0.7
0.8
0.9
Wavelength (µm)
b
Emission Intensity
Black Body
Source (3000°K)
Krypton Arc
Lamp
0.5
0.6
0.7
0.8
0.9
Wavelength (µm)
c
Emission Intensity
Diode Pump
Laser Wavelength
0.5
0.6
0.7
0.8
0.9
Wavelength (µm)

TABLE 6.2. Comparison between pumping parameters and laser wavelengths for different laser materials

	Nd:YAG	Yb:YAG	Yb:Er:glass	Cr:LISAF	Tm:Ho:YAG
Concentration	1 at.%	6.5 at.%		1 mol.%	6.5 at.% Tm 0.36 at.% Ho
Pumping diode	AlGaAs	InGaAs	InGaAs	GaInP	AlGaAs
Diode wavelength (nm)	808	950	980	670	785
Active-ion concentration [10^{20} cm^{-3}]	1.38	9	10 [Yb] 1 [Er]	0.9	8 [Tm] 0.5 [Ho]
Pump absorption coefficient (cm^{-1})	4	5	16	4.5	6
Oscillation wavelength (μm)	1.06 1.32, 1.34 0.947	1.03	1.53	0.72–0.84	2.08

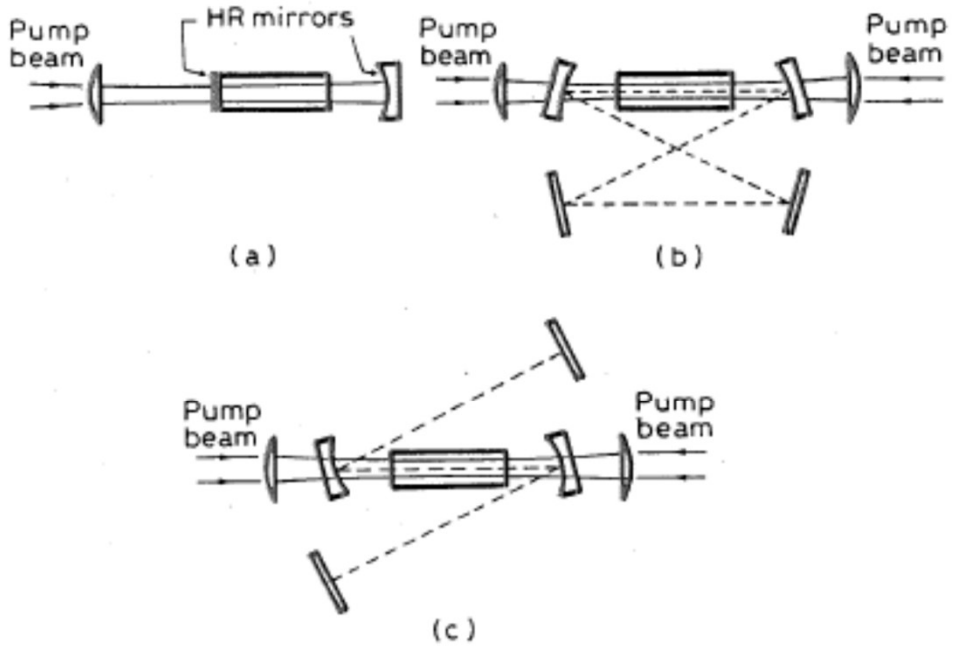

FIG. 6.11. Typical configurations for longitudinal diode laser pumping: (a) single-ended pumping in a simple plane-concave resonator, (b) double-ended pumping for a ring laser in a folded configuration, and (c) double-ended pumping for a *z*-shaped folded linear cavity.

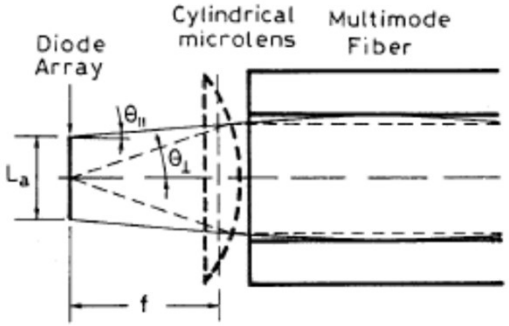

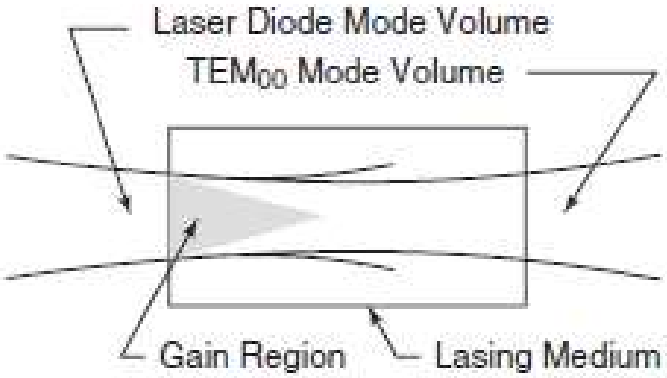

Mode Matching

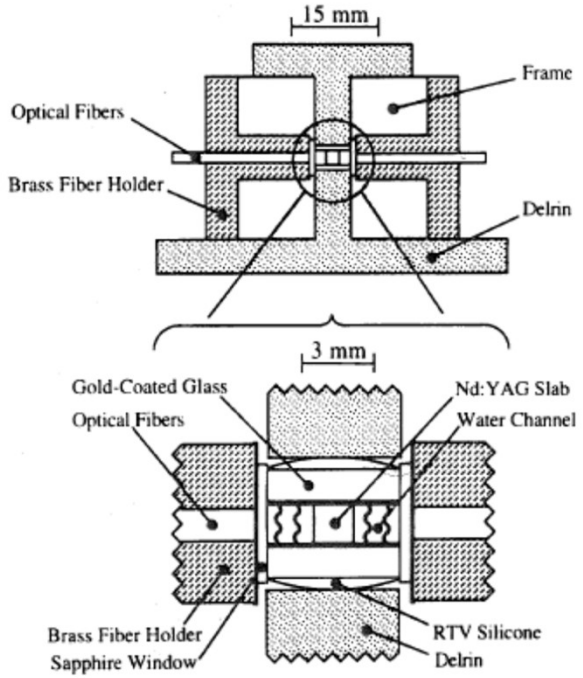

. Transverse pumping configuration for a Nd:YAG slab. (By permission from Ref. 8.)

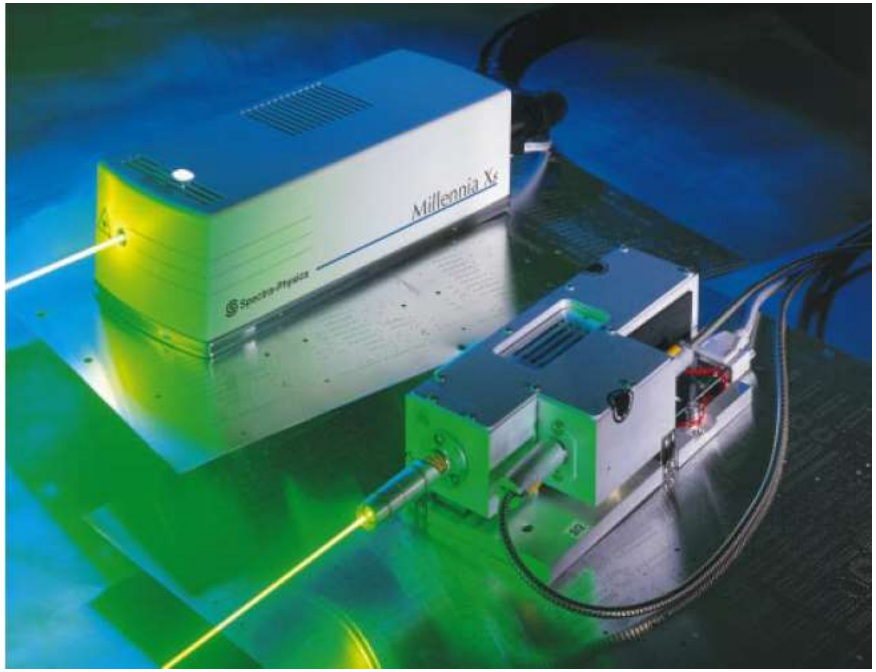

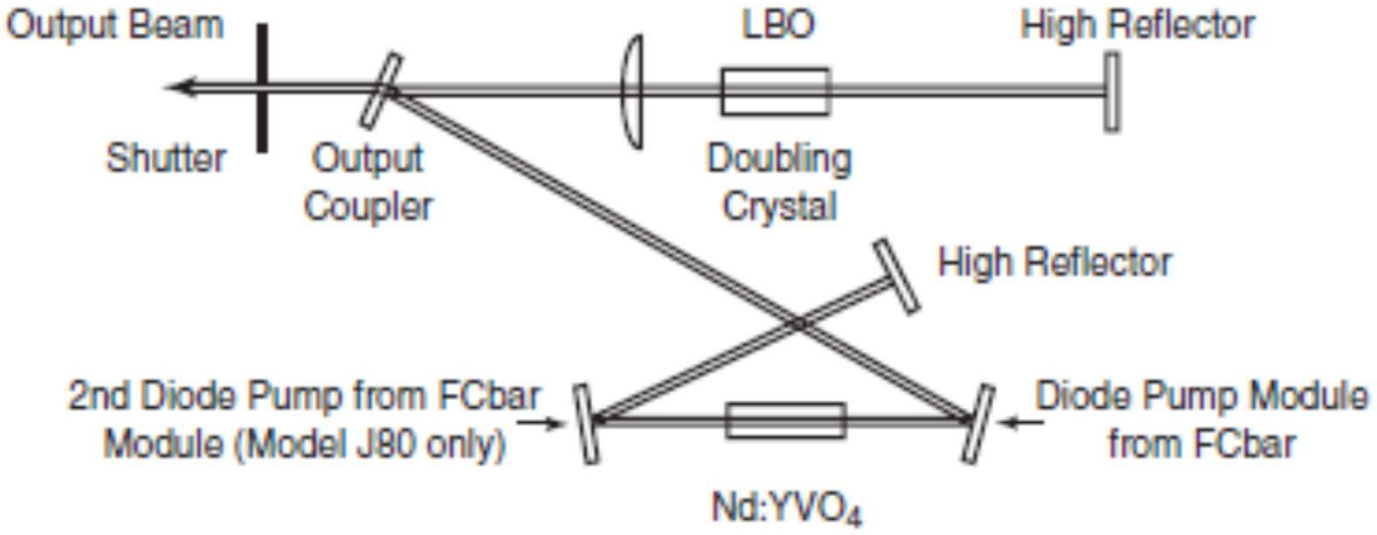

Figure 3-9: Diagram of the *Millennia Pro* Laser Head

Pevnolátkové lasery

rubín

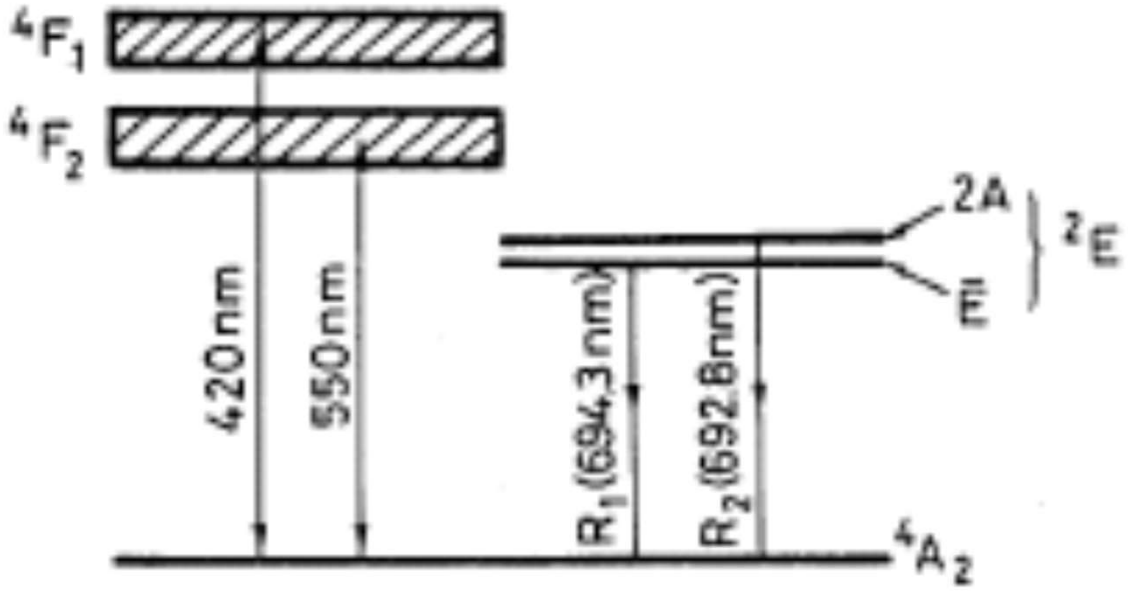

FIG. 9.1. Simplified energy levels of ruby.

TABLE 9.2. Optical and spectroscopic parameters of ruby for room temperature operation

Property	Values and Units
Cr_2O_3 doping	0.05 wt.%
Cr^{3+} concentration	1.58×10^{19} ions/cm^3
Ouput wavelengths	694.3 nm (R_1 line)
	692.9 nm (R_2 line)
Upper laser level lifetime	3 ms
Linewidth of R_1 laser transition	11 cm^{-1}
Stimulated emission cross section σ_e	2.5×10^{-20} cm^2
Absorption cross section σ_a	1.22×10^{-20} cm^2
Refractive index ($\lambda = 694.3$ nm)	$n = 1.763$ ($E \perp c$)
	$n = 1.755$ ($E \parallel c$)

Neodymové lasery

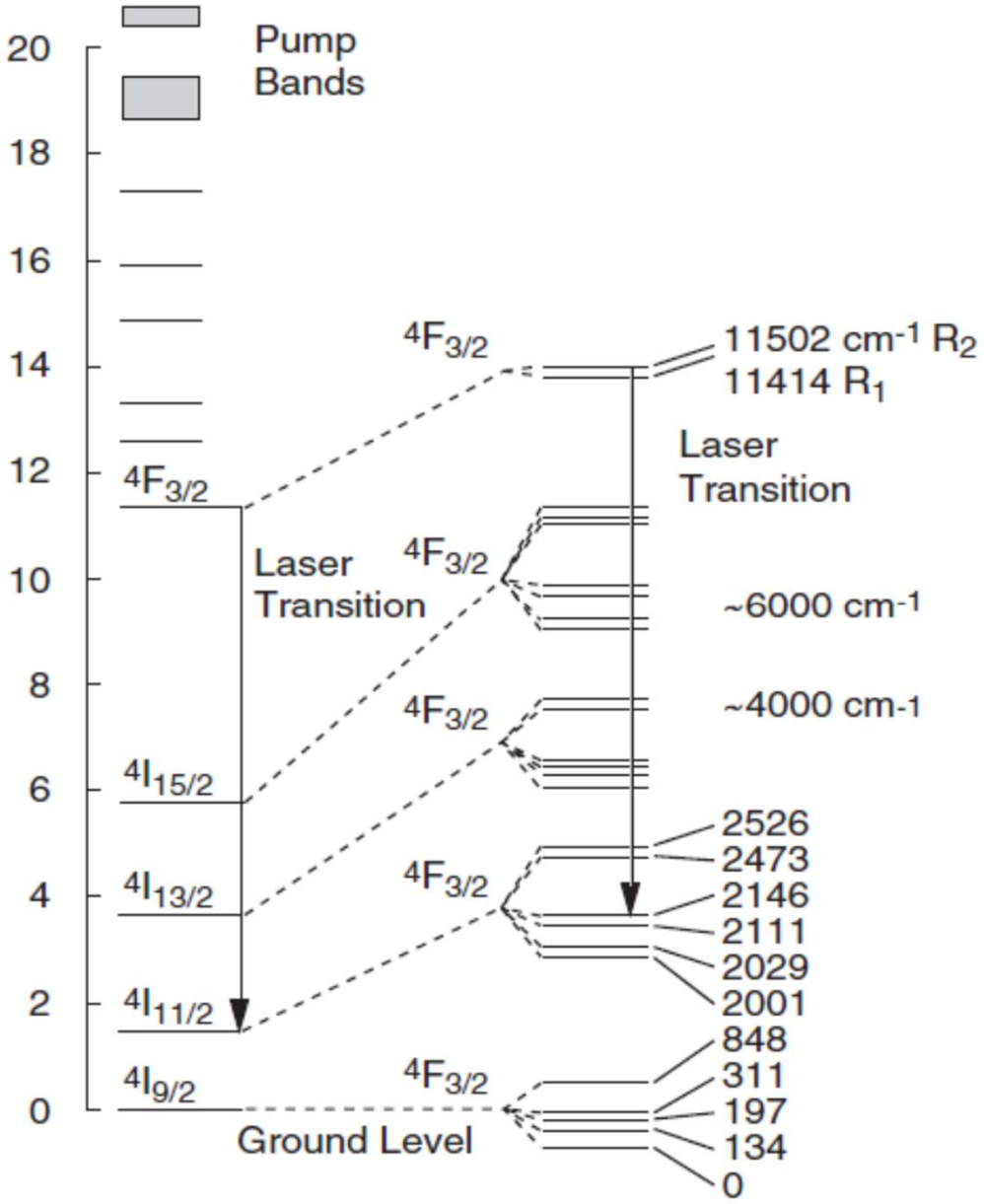

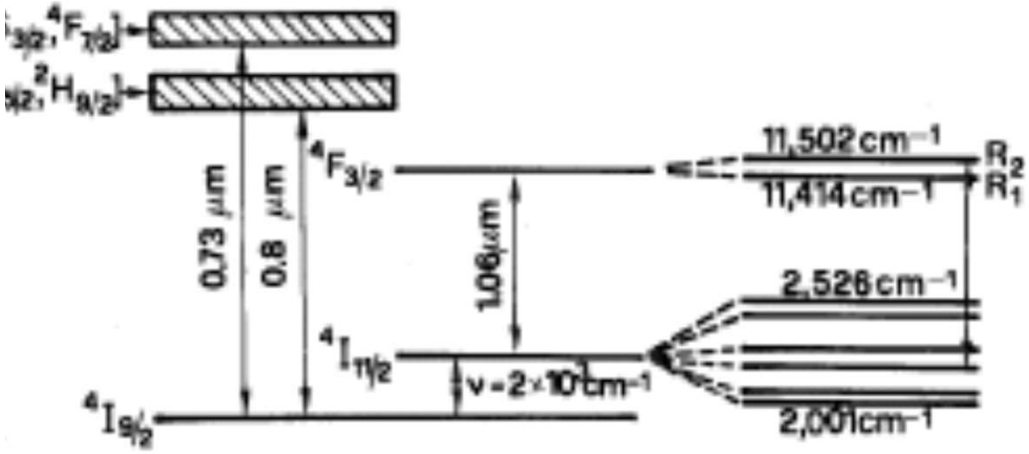

FIG. 9.2. Simplified energy levels of Nd:YAG.

TABLE 9.3. Optical and spectroscopic parameters of Nd:YAG ($\lambda = 1.064\ \mu m$), Nd:YVO_4, Nd:YLF ($\lambda = 1.053\ \mu m$), and Nd:glass (phosphate)

	Nd:YAG $\lambda = 1.064\ \mu m$	Nd:YVO_4 $\lambda = 1.064\ \mu m$	Nd:YLF $\lambda = 1.053\ \mu m$	Nd:glass $\lambda = 1.054\ \mu m$ (Phosphate)
Nd doping	1 atom.%	1 atom.%	1 atom.%	3.8% by weight of Nd_2O_3
N_t (10^{20} ions/cm^3)[a]	1.38	1.5	1.3	3.2
τ (μs)[b]	230	98	450	300
$\Delta\nu_0$ (cm^{-1})[c]	4.5	11.3	13	180
σ_e (10^{-19} cm^2)[d]	2.8	7.6	1.9	0.4
Refractive index	$n = 1.82$	$n_o = 1.958$ $n_e = 2.168$	$n_o = 1.4481$ $n_e = 1.4704$	$n = 1.54$

[a] N_t is the concentration of the active ions, [b] τ is the fluorescence lifetime, [c] $\Delta\nu_0$ is the transition linewidth (FWHM), [d] σ_e is the effective stimulated emission cross section. Data refer to room temperature operation.

$YLiF_4$ (YLF) and YVO_4.

TABLE 9.4. Optical and spectroscopic parameters at room temperature of the most important quasi-three-level laser materials

Active Medium Parameters	Yb:YAG $\lambda = 1.03\ \mu m$	Nd:YAG $\lambda = 946\ \mu m$	Tm:Ho:YAG $\lambda = 2.091\ \mu m$	Yb:Er:Glass[a] $\lambda = 1.54\ \mu m$ (Phosphate)
Doping (atom.%)	6.5 atom.	1.1 atom.		
N_r (10^{20} ions/cm^3)	8.97	1.5	8 (Tm) 0.5 (Ho)	10 (Yb) 1 (Er)
τ (ms)	1.16	0.23	8.5	8
$\Delta\nu_0$ (cm^{-1})	86	9.5	42	120
σ_e (10^{-20} cm^2)	1.8	2.4	0.9	0.8
σ_a (10^{-20} cm^2)	0.12	0.296	0.153	0.8
Refractive index	$n = 1.82$	$n = 1.82$	$n = 1.82$	$n = 1.531$

[a] For Yb:Er:glass, the effective value of the stimulated emission and absorption cross sections are about the same, so the laser can be considered to operate in (almost) a pure three-level scheme.

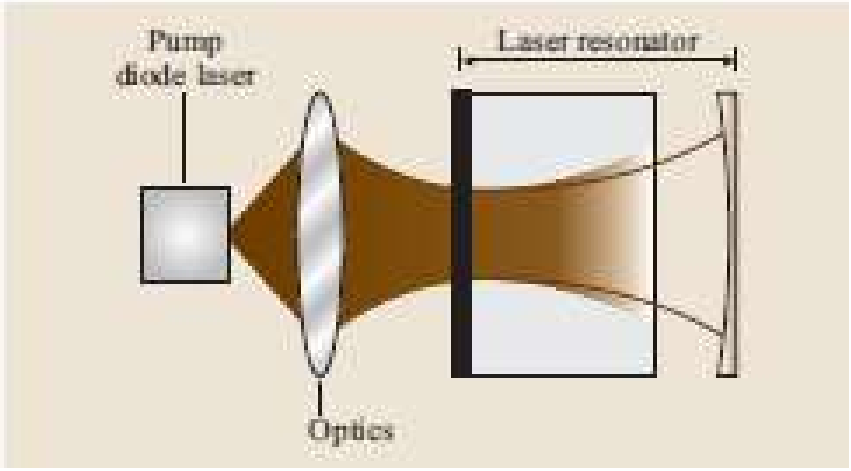

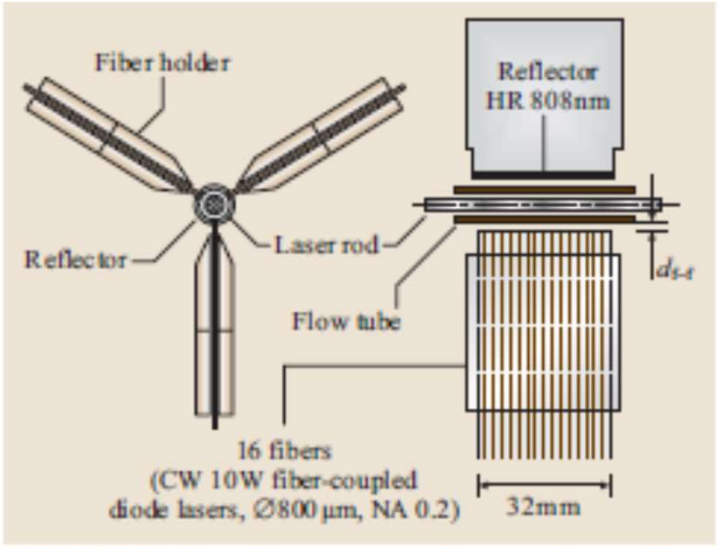

Fig. 11.53 Diode side (transversal) pumping scheme [11.266]

Table 11.22 Overview of Ti^{3+}:Al_2O_3 laser-relevant parameters [11.948, 950]

Index of refraction	1.76
Absorption cross section	6.5×10^{-20} cm^2 ($E \parallel c$)
Fluorescence lifetime	3.2 µs
Fluorescence bandwidth (FWHM)	≈ 200 nm
Peak emission wavelength	790 nm
Peak stimulated emission cross section	4.1×10^{-19} cm^2 ($E \parallel c$)
	2.0×10^{-19} cm^2 ($E \perp c$)
Quantum efficiency	≈ 0.9–1
Saturation fluence	0.9 J/cm^2
Dopant concentration	0.1% (weight)
Growth	Czochralski, heat exchange
T_m	2050 °C
Thermal conductivity	28 W/mK
Thermal lens (dn/dT)	12×10^{-19} K^{-1}

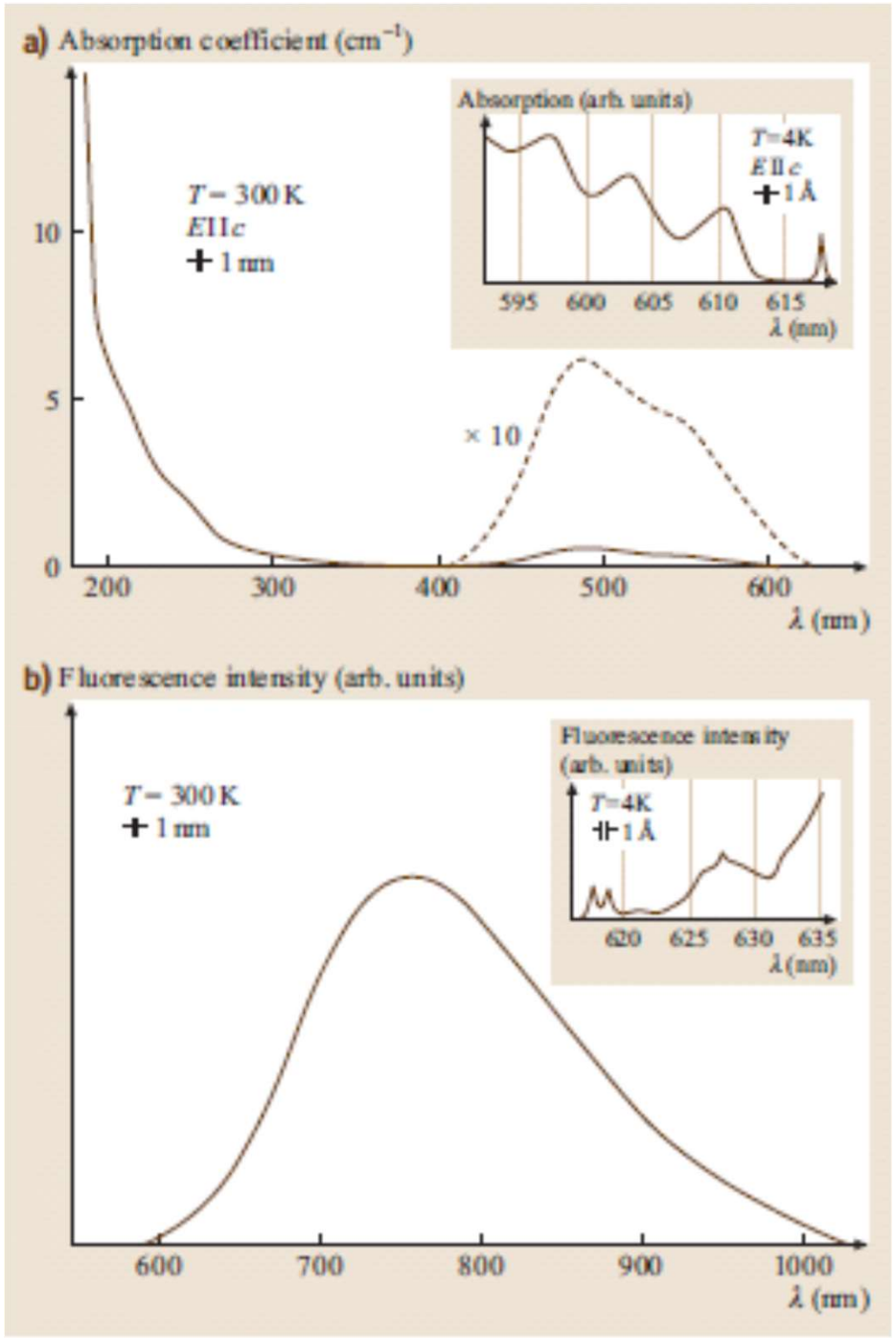

Fig. 11.80a,b Absorption (a) and emission (b) spectra at room temperature and at 4 K of Ti:sapphire. (After [11.948])

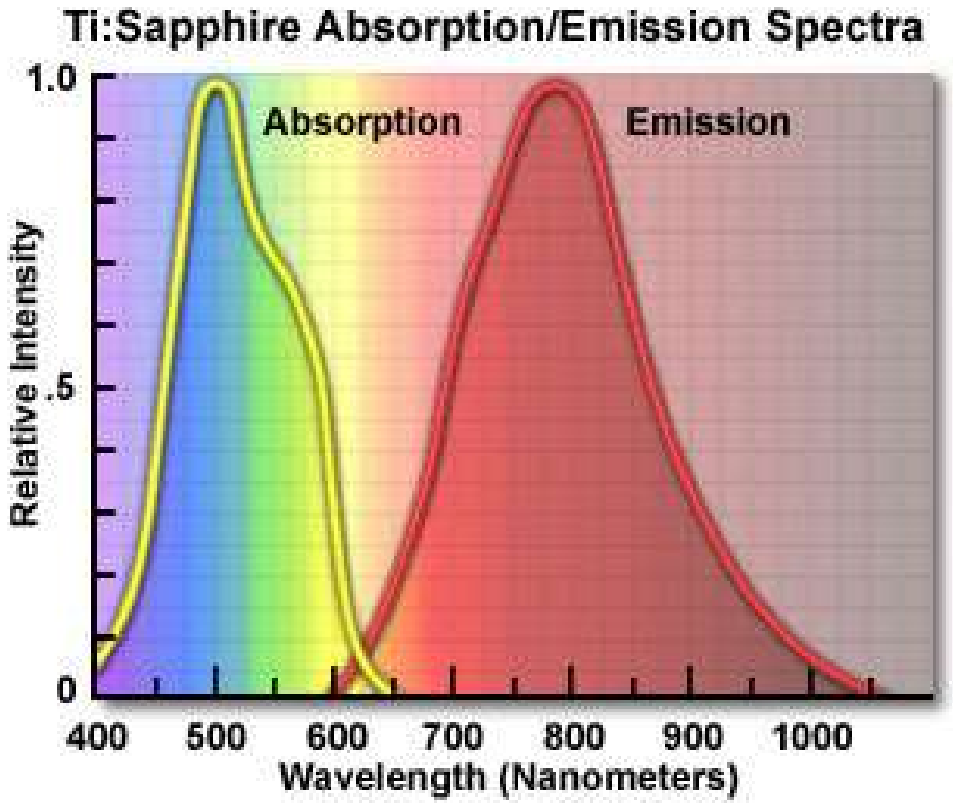
Ti:Sapphire Absorption/Emission Spectra
1.0
.5
0
Relative Intensity
Absorption
Emission
400
500
600
700
800
900
1000
Wavelength (Nanometers)

Figure 1

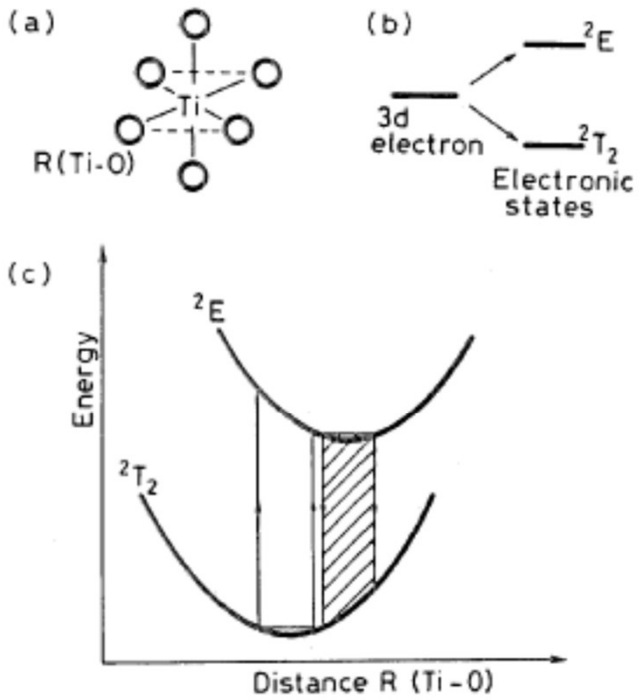

FIG. 9.9. (a) Octahedral configuration of $Ti:Al_2O_3$, (b) splitting of $3d$ energy states in an octahedral crystal field, and (c) energy states in a configuration coordinate model.

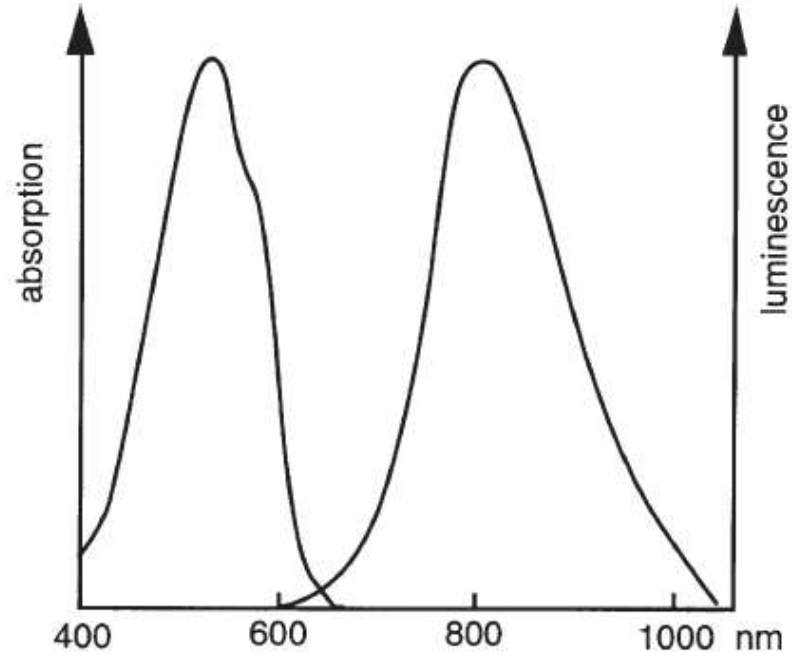

Fig. 4.15. Normalized absorption and emission spectra of Ti^{3+} ions embedded as impurities in a sapphire matrix ($Ti:Al_2O_3$)

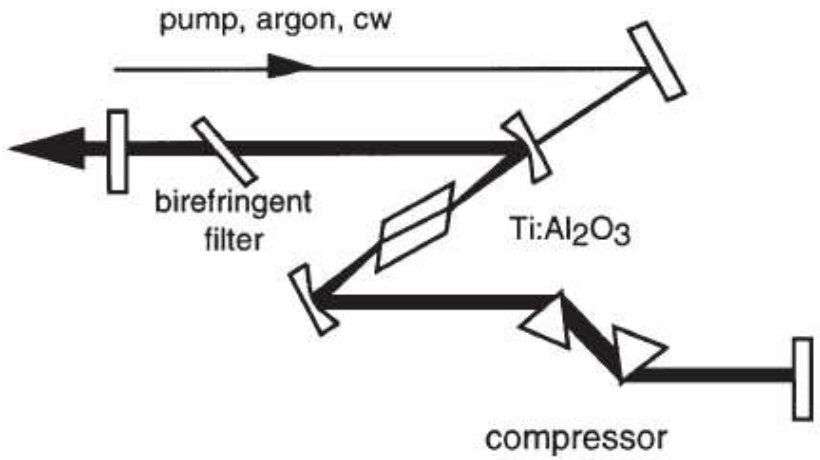

Fig. 4.16. Simplified sketch of a Ti:sapphire laser

Cavity configuration of fsTi:Sapphire laser

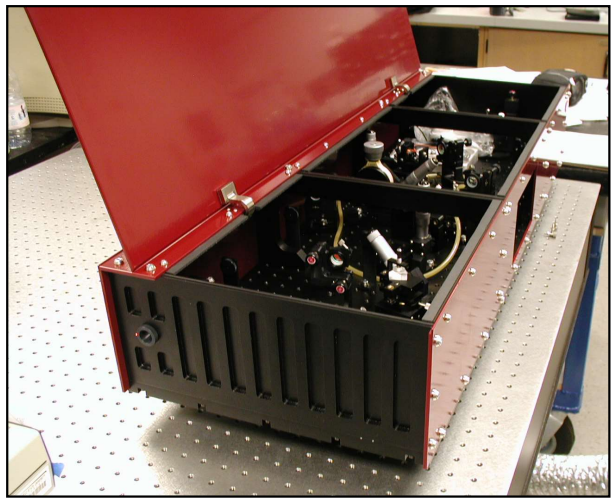

Tuning range 700-1000 nm
Pulse duration < 20 fs
Pulse energy < 10 nJ
Repetition rate 80 – 1000 MHz
Pump power: 2-15 W

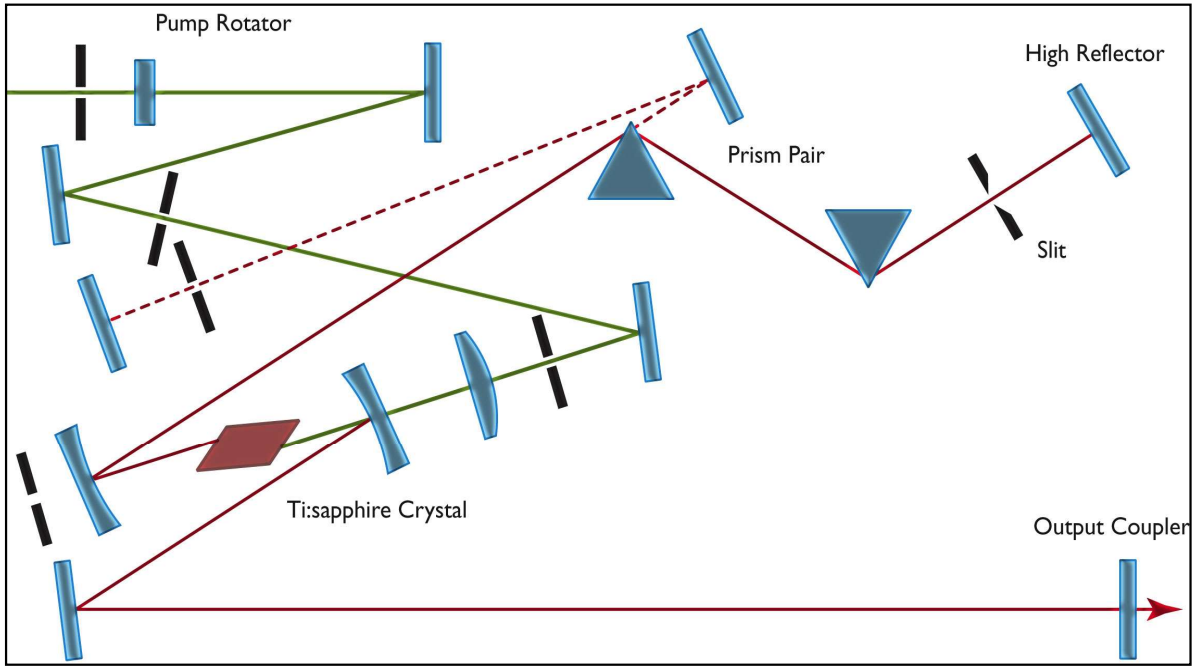

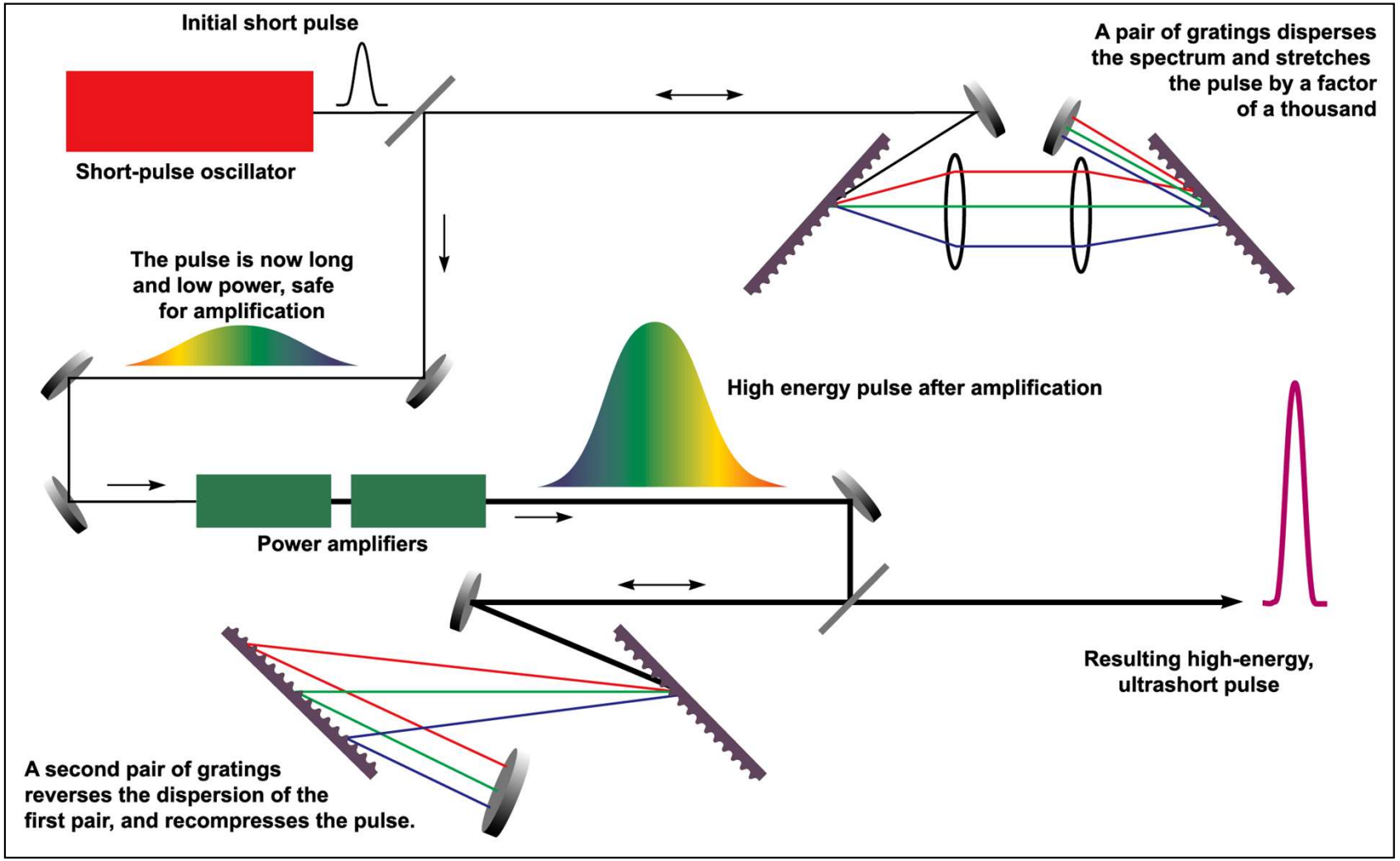
Initial short pulse
Short-pulse oscillator
A pair of gratings disperses the spectrum and stretches the pulse by a factor of a thousand
The pulse is now long and low power, safe for amplification
High energy pulse after amplification
Power amplifiers
Resulting high-energy, ultrashort pulse
A second pair of gratings reverses the dispersion of the first pair, and recompresses the pulse.

FREE ELECTRON LASER – LASER NA VOLNÝCH ELEKTRONECH

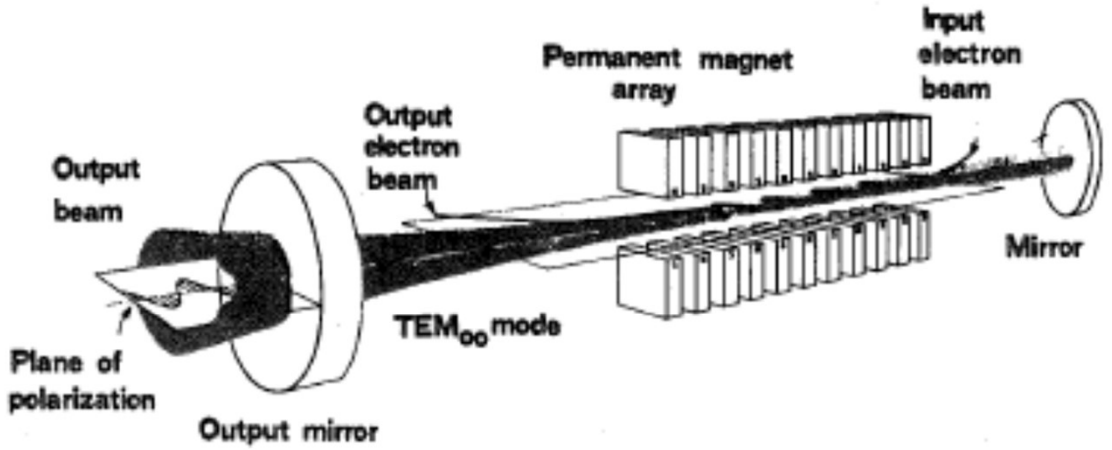

FIG. 10.24. Basic structure of a free-electron laser. (Courtesy of Luis Elias, University of California, at Santa Barbara Quantum Institute.)

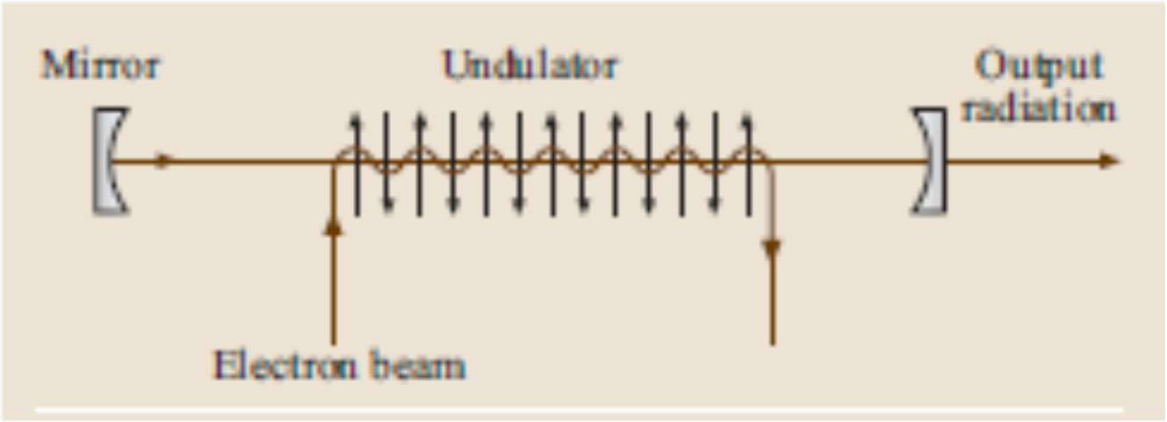

Table 11.53 Parameter space of free-electron lasers as of 2006

Radiation	
Wavelength	13 nm–10 mm
Peak power	up to 5 GW
Average power	up to 10 kW
Pulse duration	10 fs to CW
Driving electron beam	
Energy	200 keV–1 GeV
Peak current	1–3000 A
Undulator	
Period	0.5–20 cm
Peak magnetic field	0.1–1 T
Undulator length	0.5–27 m

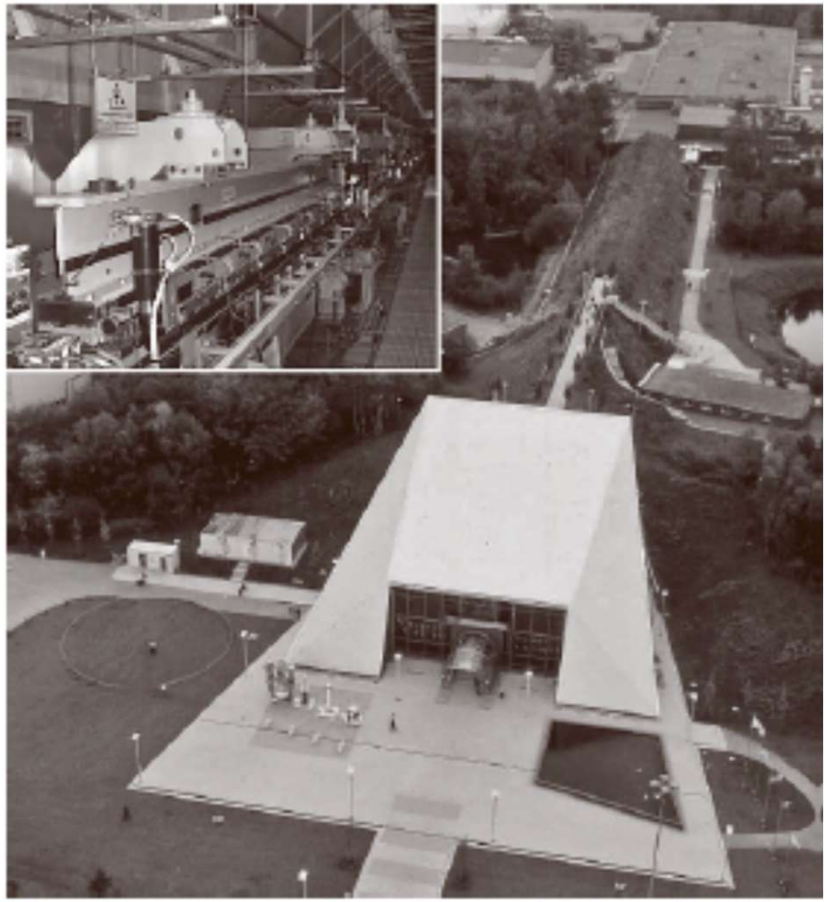

Fig. 11.212 Aerial view of the experimental hall for the FLASH user facility in Hamburg (*center*) and the tunnel for the superconducting accelerator and undulator (*covered with grass*). The hall in the upper right corner houses the injector part of the linac. The total length of the FLASH facility is 300 m. The maximum energy of electrons is 1 GeV, and the minimum radiation wavelength is 6 nm. The undulator of the FLASH (photo in the *upper left corner*) is a permanent magnet device (period 2.73 cm, gap 12 mm, peak field 0.47 T). The undulator system is subdivided into six segments, each 4.5 m long

RTG LASERY

	2006: FLASH	2013: European XFEL
Radiation		
Wavelength	13–180 nm	down to 0.1 nm
Peak power	up to 5 GW	up to 150 GW
Average power	10 mW	up to 500 W
Pulse duration	10–50 fs	0.2–100 fs
Driving electron beam		
Energy	0.3–0.7 GeV	up to 20 GeV
Peak current	1–3 kA	up to 5 kA
Undulator		
Period	2.73 cm	3.6–8 cm
Peak magnetic field	0.5 T	0.5–1.4 T
Undulator length	27 m	up to 200 m

JINÉ RTG LASERY

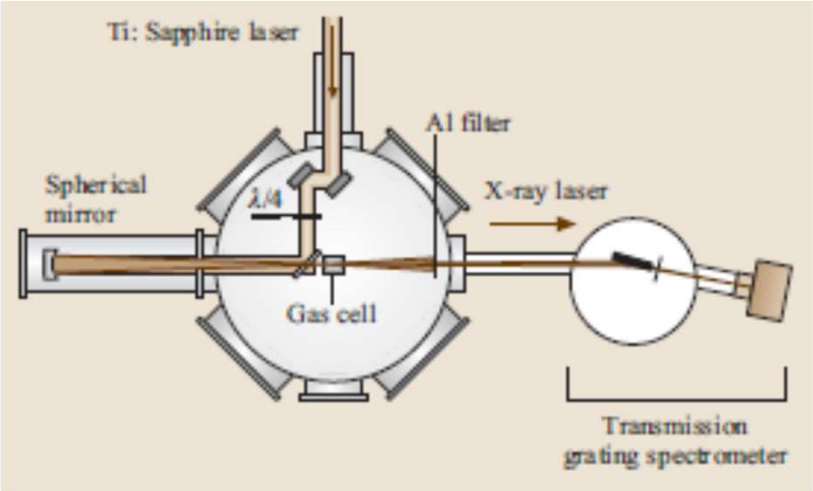

Fig. 11.222 Schematic diagram of the experimental setup of optical-field ionization X-ray laser based on electron collision excitation

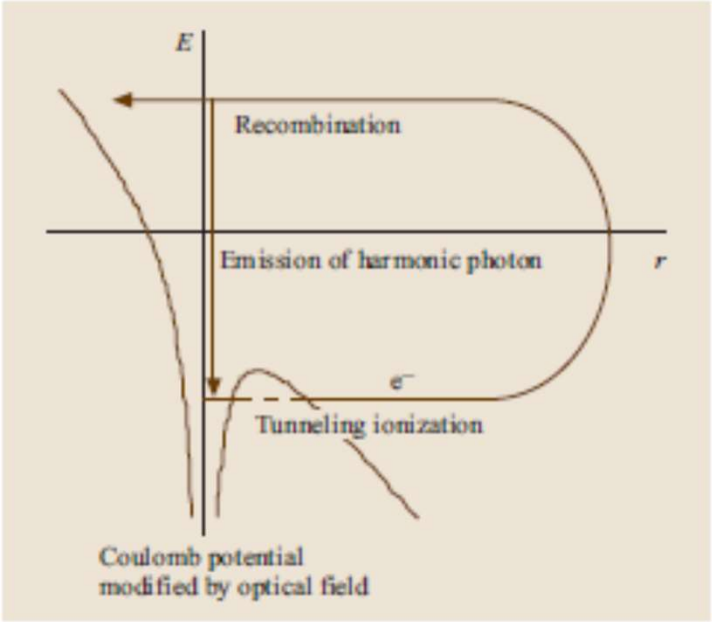

Fig. 11.226 Schematic drawing of a semiclassical model of high-order-harmonic generation

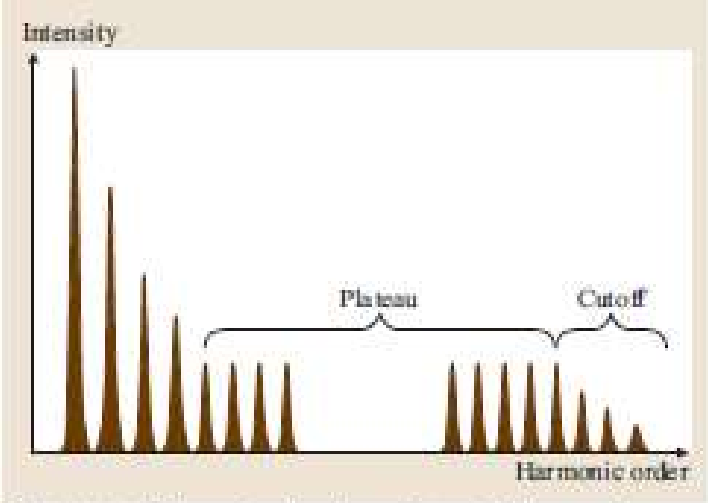

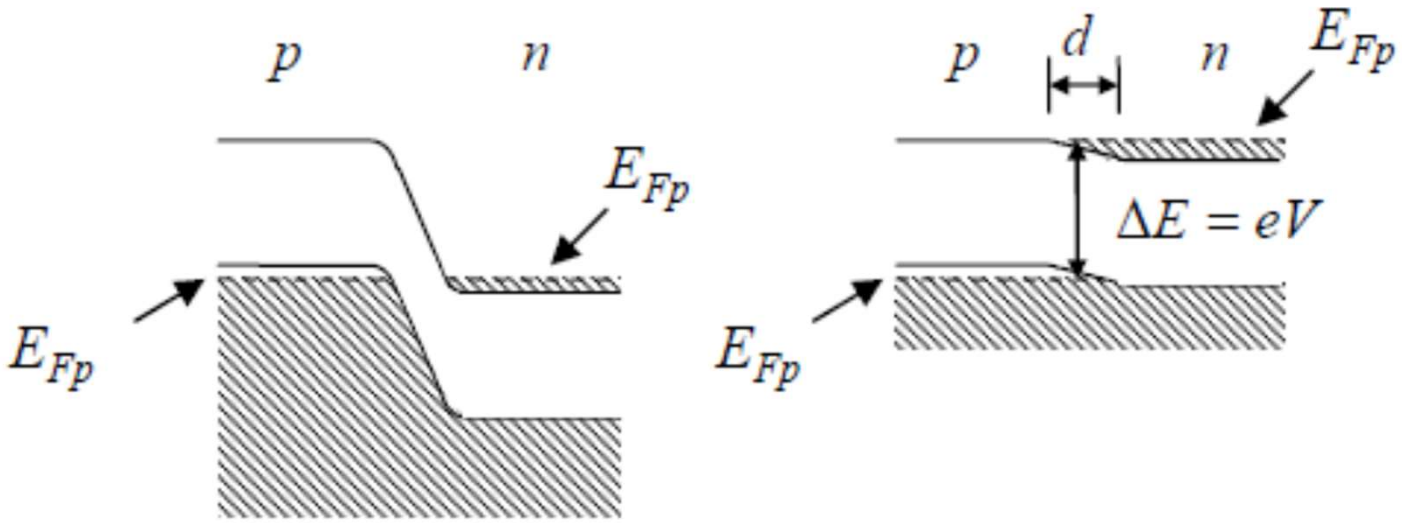

P-n přechod

Polovodičový laser

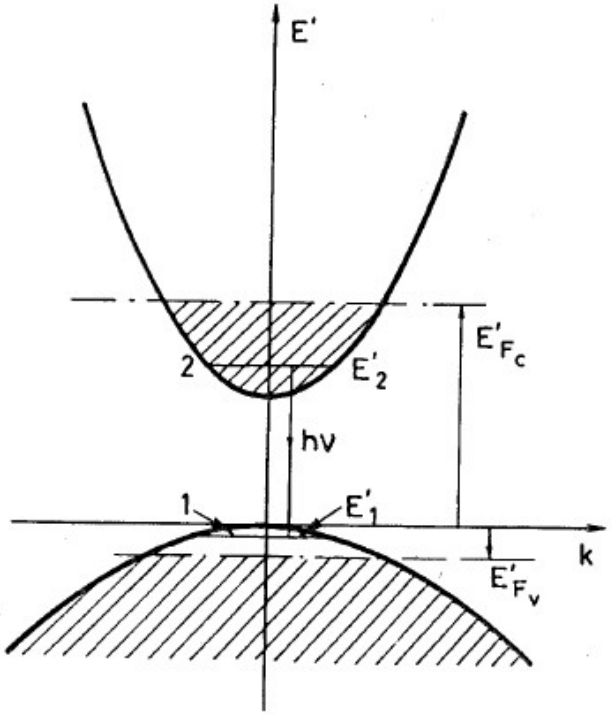

Graphical illustration of the Bernard–Duraffourg condition for achieving net gain

$$E_g \leq h\nu \leq E'_{F_c} - E'_{F_v}$$

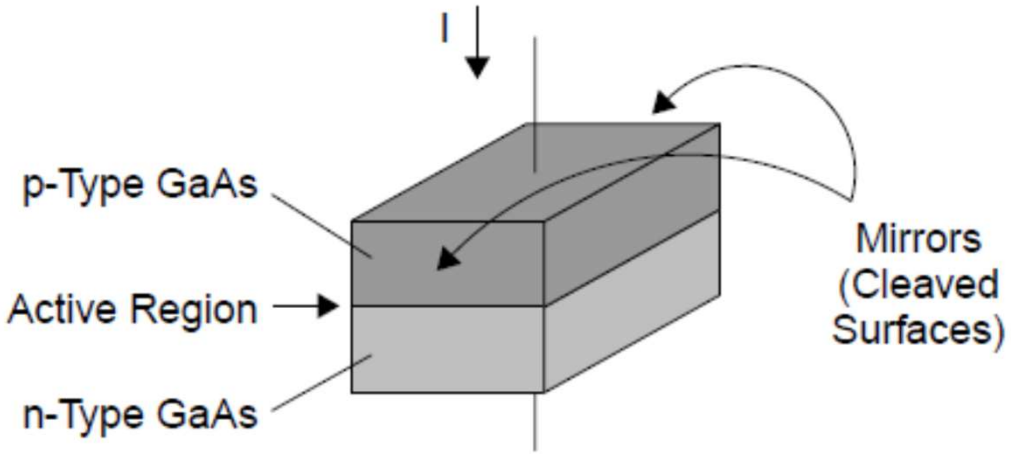

Homojunction laser structure

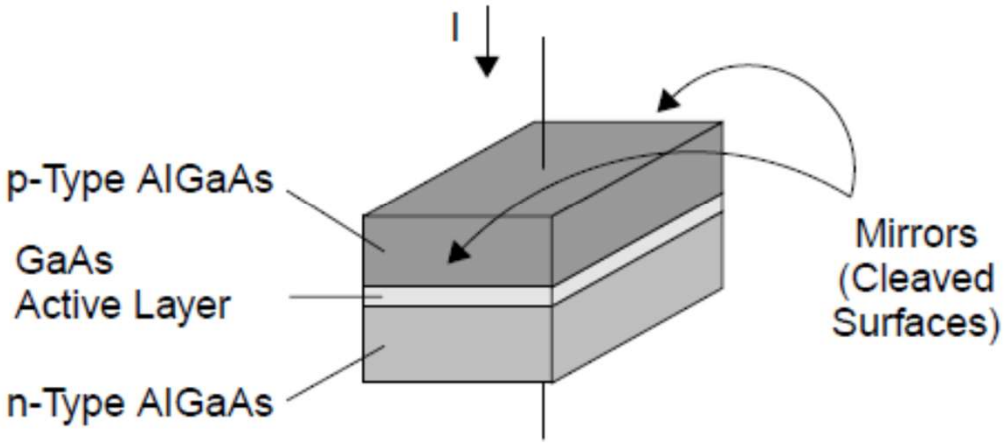

Heterojunction laser structure.

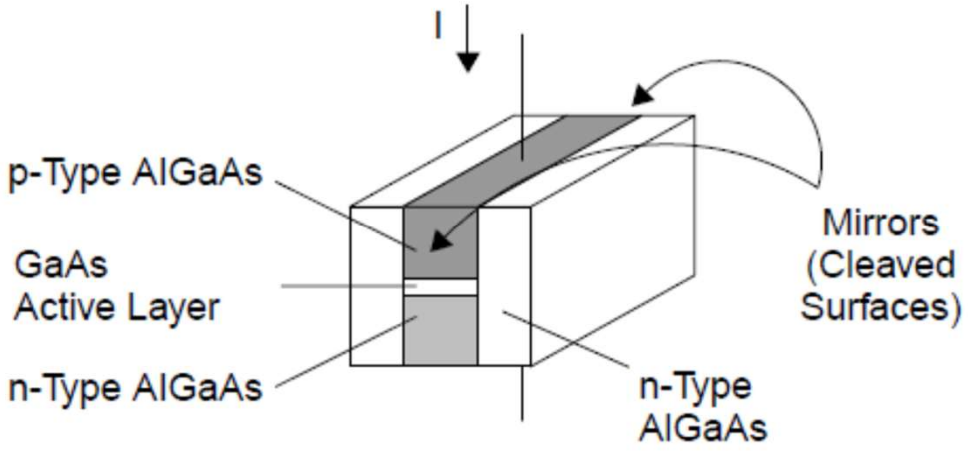

Buried heterojunction laser structure.

405 nm – InGaN blue-violet laser, in Blu-ray Disc and HD DVD drives

657 nm – AlGaInP DVD drives, laser pointers

785 nm – GaAlAs Compact Disc drives

1550 nm – InGaAsP fiber-optic communication